5. Optical Resonators

Optical resonators are, to a large extent, responsible for the unique properties of the radiation emitted by lasers. The simplest kind of resonator is a so-called Fabry-Perot resonator. It consists of two mirrors facing each other, centered with respect to a common optical axis and placed perpendicular to it.

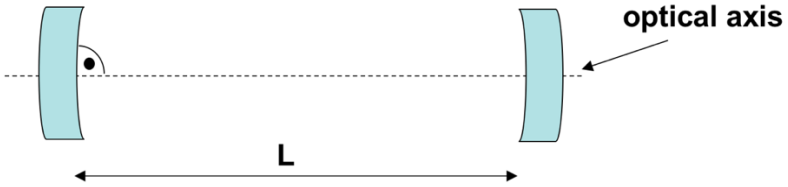

In chapter 3 it has been stated that self-consistency after each resonator round-trip is an essential condition for stationary laser operation. As a direct consequence of this condition, there are eigen-frequencies corresponding to longitudinal / axial modes, which need to fulfil the following relation:

$$L = q \cdot \frac{\lambda}{2}$$

with L being the mirror separation (length of the resonator) and q being an integer (mode order). The eigen-frequencies in such a linear cavity are, therefore, given by:

$$\nu_q = q \cdot \frac{c}{2 \cdot L}$$

hence, their frequency separation is

$$\Delta\nu_q = \nu_q - \nu_{q-1} = \frac{c}{2 \cdot L}$$

At this point it is worth recalling that the essential condition for starting laser oscillation was that the yield (per round-trip) is larger than the losses (also per round-trip), i.e.:

$R \cdot V \cdot G_0 \geq 1$

with G_0 representing the small signal gain factor, R the reflectivity of the out-coupling mirror and V being the parameter encompassing all other losses. If we assume that R and V are not frequency dependent, then the frequency range which fulfills $R \cdot V \cdot G_0 \geq 1$ is determined solely by the linewidth of the laser transition.

As an example: A cavity length L of 30 cm results in a frequency separation of the longitudinal modes as high as 500 MHz. Taking into account that the linewidth of the 633 nm transition in a HeNe-laser is about 1.5 GHz, only 3 longitudinal modes might be able to start oscillating. On the other hand, Ruby possesses a linewidth of 330 GHz and, thus, more than 500 longitudinal modes can fulfill the condition yield>losses in this resonator.

We also know that each beam has a finite divergence as it propagates. Therefore, it can be expected that a plane-plane Fabry-Perot resonator exhibits high losses (as the beam keeps on expanding with each round-trip). In order to obtain lower losses it would be beneficial to concentrate the rays close to the optical axis. This is something that can potentially be done by using curved mirrors. The feasibility of this approach is studied in the next section using ray-optics.

5.1 Ray Optical consideration of Laser Resonators

In this section we consider Fabry-Perot resonators within the scope of geometrical optics (by means of a ray transfer-matrix analysis also known as ABCD matrix analysis). In doing so diffraction effects are disregarded. The goal of this analysis is to derive the criteria of stability of laser resonators.

We assume that the rays propagate in the z-direction and that the rays have a small separation r(z) to the z-axis (optical axis). In addition, the rays also propagate with a small angle relative to the z-axis (i.e. its propagation slope *r'* has to be small). This is the so-called paraxial approximation. Mathematically the slope of the ray is described by:

$$r' = \frac{dr}{dz}$$

The ABCD-matrix analysis allows calculating how *r* and *r'* change during propagation or after interaction with optical elements. In the following we will set that formalism up by considering a few simple examples.

A) propagation in vacuum

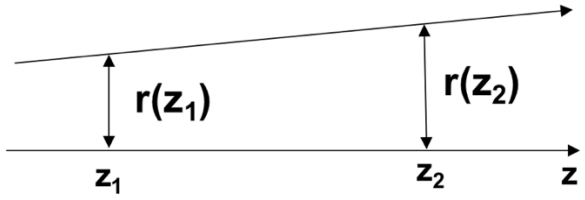

Let's assume that *r* and *r'* are given at position z_1:

$r_1 = r(z_1)$ and $r_1' = r'(z_1)$

then, at position z_2 :

$$r_2 = r_1 + (z_2 - z_1) \cdot r_1' \qquad (5.1a)$$

i.e. the ray propagates in a straight line as the propagation slope is conserved:

$$r_2' = r_1' \qquad (5.1b)$$

B) passing through an even interface (interface perpendicular to the optical axis)

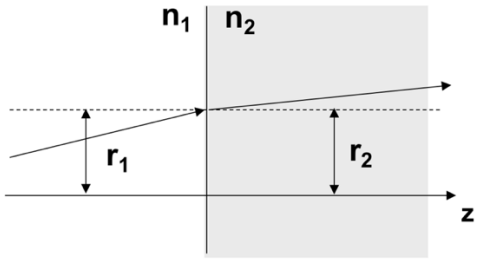

Within the paraxial approximation r and r' are small in the optical system. Therefore, right before and after the interface the distance to the optical axis is the same:

$r_2 = r_1$ (5.2)

However, if the interface separates media with different refractive indexes, the beam will be refracted. The change of propagation direction of the ray (slope) is described by Snell's law of refraction in the paraxial approximation:

$n_2 \cdot r_2' = n_1 \cdot r_1'$ (5.3)

C) passing through a thin lens with focal length f

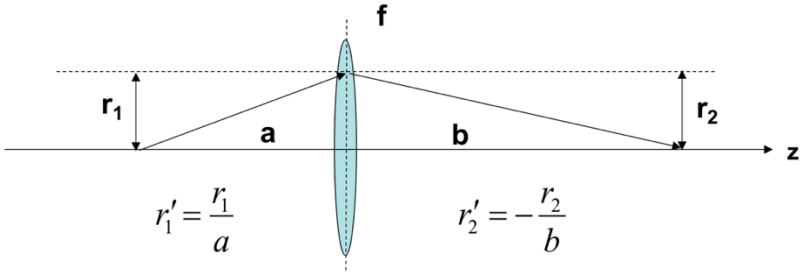

At the position (dashed vertical line in the figure above) of the lens the distance of the beam to the optical axis remains unchanged. Hence,

$r_2 = r_1$.

The position of the image is described by the lens law, which provides the relation between the distances a, b and the focal length of the lens f:

$$\frac{1}{a} + \frac{1}{b} = \frac{1}{f}$$

Using the lens law and the relations given in the figure, it is possible to calculate the change of the propagation direction of the beam induced by the lens as:

$$r_2' = r_1' - \frac{r_1}{f}.$$ (5.4)

In general, the effect of an optical element on the beam can be written as:

$$\begin{aligned} r_2 &= Ar_1 + Br_1' \\ r_2' &= Cr_1 + Dr_1' \end{aligned} \qquad (5.5a)$$

And, therewith, the interaction of a beam with optical elements can be summarized in an elegant matrix formalism. For this, it is necessary to define the ray vector and the ray matrix as:

$$\underline{r}_i = \begin{pmatrix} r_i \\ r_i' \end{pmatrix} \qquad \underline{\underline{M}} = \begin{pmatrix} A & B \\ C & D \end{pmatrix}$$

Using this formulation it is possible to describe the evolution of the ray (i.e. distance to optical axis and propagation slope with respect to it) by multiplying the ray matrix with the ray vector before the element:

$$\underline{r}_2 = \underline{\underline{M}} \cdot \underline{r}_1 \qquad (5.5b)$$

Thus, using this formalism, the ray matrices for the different optical elements discussed above can be easily stated:

A) propagation of a distance L in vacuum

$$\underline{\underline{M}} = \begin{pmatrix} 1 & L \\ 0 & 1 \end{pmatrix} \qquad (5.6a)$$

B) passing through a plane/flat interface

$$\underline{\underline{M}} = \begin{pmatrix} 1 & 0 \\ 0 & n_1 / n_2 \end{pmatrix} \qquad (5.6b)$$

C) passing through a thin lens

$$\underline{\underline{M}} = \begin{pmatrix} 1 & 0 \\ -\frac{1}{f} & 1 \end{pmatrix} \qquad (5.6c)$$

D) reflection on a spherical mirror having radius of curvature R (convention: R > 0, if ray hits a concave surface)

$$\underline{\underline{M}} = \begin{pmatrix} 1 & 0 \\ -\frac{2}{R} & 1 \end{pmatrix} \qquad (5.6d)$$

The advantage of the matrix formalism is that more elements can be incorporated by simple algebra. Considering two elements M^1 and M^2 and a starting ray vector r_0, the ray vector after propagation through these two elements is given by:

$$\underline{r}_1 = \underline{\underline{M}}^1 \cdot \underline{r}_0$$
$$\underline{r}_2 = \underline{\underline{M}}^2 \cdot \underline{r}_1 = \underline{\underline{M}}^2 \cdot \left(\underline{\underline{M}}^1 \cdot \underline{r}_0\right) \qquad (5.7)$$

Thus, the effect of the two elements can be summarized by the matrix product:

$$\underline{r}_2 = \underline{\underline{M}} \cdot \underline{r}_0 \quad with \quad \underline{\underline{M}} = \underline{\underline{M}}^2 \cdot \underline{\underline{M}}^1$$

It is important to note that the matrix product is not commutative, i.e. it is necessary to respect the order of the optical elements in the setup.

Fabry-Perot Resonator

As mentioned before, a Fabry-Perot resonator consists of two mirrors with radii of curvature R_1 and R_2 facing each other and separated by a distance L.

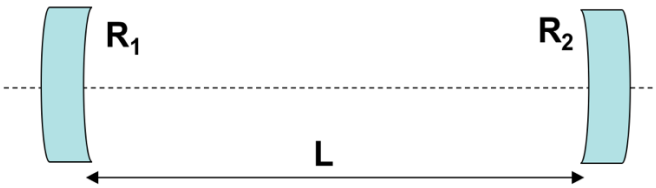

Using equations (5.6 c) and (5.6 d) it can be inferred that the effect of a spherical mirror with radius of curvature R is equivalent to that of a lens with focal distance R/2. Hence, instead of the mirror arrangement, we can consider a system of lenses each separated by a distance L with focal lengths

$$f_1 = \frac{R_1}{2} \quad \text{and} \quad f_2 = \frac{R_2}{2}.$$

This substitution results in a so-called lens guide:

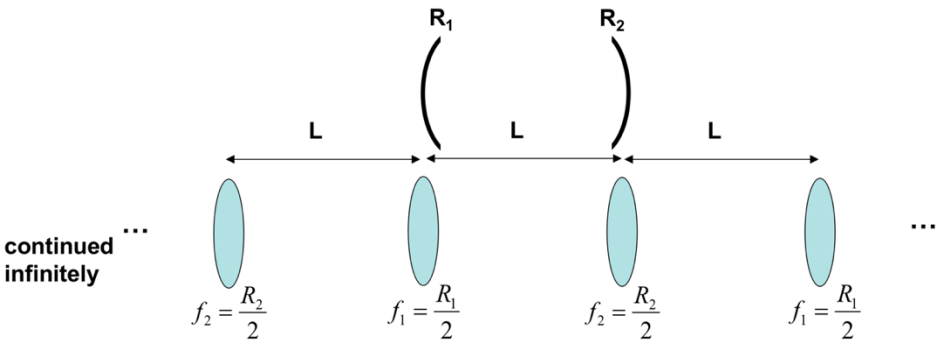

As can be seen, a lens guide is formed through the repetition of a basic unit, as illustrated below:

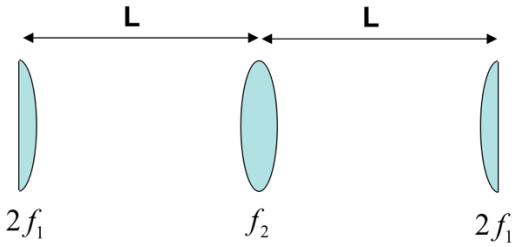

Using the matrix formalism introduced above it is possible to describe the effect of the basic unit:

$$\begin{pmatrix} r_1 \\ r_1' \end{pmatrix} = \begin{pmatrix} 1 & 0 \\ -\frac{1}{2f_1} & 1 \end{pmatrix} \cdot \begin{pmatrix} 1 & L \\ 0 & 1 \end{pmatrix} \cdot \begin{pmatrix} 1 & 0 \\ -\frac{1}{f_2} & 1 \end{pmatrix} \cdot \begin{pmatrix} 1 & L \\ 0 & 1 \end{pmatrix} \cdot \begin{pmatrix} 1 & 0 \\ -\frac{1}{2f_1} & 1 \end{pmatrix} \cdot \begin{pmatrix} r_0 \\ r_0' \end{pmatrix} \tag{5.8}$$

In order to get dimensionless matrix elements, the ray vector can be re-defined as:

$$\underline{r}_i = \begin{pmatrix} r_i \\ L \cdot r_i' \end{pmatrix}. \tag{5.9a}$$

Furthermore, we also define the resonator parameters g_1 and g_2 as

$$g_i = 1 - \frac{L}{R_i}, \tag{5.9b}$$

which allows re-writing the focal length as:

$$f_i = \frac{R_i}{2} = \left(\frac{L}{2}\right) \cdot (1 - g_i)^{-1} \tag{5.9c}$$

With these definitions, and performing the matrix multiplication in equation (5.8), the matrix of the basic unit is given by:

$$\underline{r}_1 = \begin{pmatrix} 2g_1g_2 - 1 & 2g_2 \\ 2g_1(g_1g_2 - 1) & 2g_1g_2 - 1 \end{pmatrix} \cdot \underline{r}_0 = \underline{\underline{M}} \cdot \underline{r}_0 . \tag{5.10}$$

This matrix governs the evolution of the ray parameters after one round-trip. To describe the back-and-forth bouncing of a beam in a resonator (i.e. the different round-trips), we need to apply the matrix of the basic unit n-times:

$$\underline{r}_n = \underline{\underline{M}} \cdot \underline{\underline{M}} \cdot \underline{\underline{M}} \cdot \underline{\underline{M}} \cdot \ldots \cdot \underline{\underline{M}} \cdot \underline{r}_0 = \left(\underline{\underline{M}}\right)^n \cdot \underline{r}_0 . \tag{5.11a}$$

In a resonator n has to approach infinity:

$$\underline{r}_{\infty} = \lim_{n\to\infty} \left(\underline{\underline{M}}\right)^{n} \cdot \underline{r}_{0} \tag{5.11b}$$

However, direct matrix multiplication is not an effective approach to calculate this limit. One workaround is the investigation of special ray vectors, known as the eigenvectors r_e of the optical system, which are defined by:

$$\underline{\underline{M}} \cdot \underline{r}_{e} = \mathrm{I} \cdot \underline{r}_{e} \tag{5.12a}$$

where λ is the eigenvalue (real quantity) associated to the eigenvector r_e. Repeated propagation (n-times) of the eigenvectors through the basic unit is represented by:

$$\left(\underline{\underline{M}}\right)^{n} \cdot \underline{r}_{e} = \mathrm{I}^{n} \cdot \underline{r}_{e} \tag{5.12b}$$

By transforming that expression into an eigenvalue equation (i.e. a set of linear homogeneous equations), and setting the determinant of the coefficient matrix to 0, it is possible to obtain a characteristic polynomial, which allows calculating the eigenvalues $\lambda_{a,b}$:

$$\mathrm{I}_{a,b} = \left(2 \cdot g_1 \cdot g_2 - 1\right) \pm \sqrt{4 \cdot g_1 \cdot g_2 \cdot \left(g_1 \cdot g_2 - 1\right)} \tag{5.12c}$$

The associated eigenvectors r_a and r_b are linearly independent and, hence, it is possible to construct of any vector by a linear combination of them, such as:

$$\underline{r}_{0} = C_a \cdot \underline{r}_{a} + C_b \cdot \underline{r}_{b} \tag{5.13a}$$

Therefore, after n passes through the basic unit the resulting ray vector can be expressed as:

$$\underline{r}_{n} = \left(\underline{\underline{M}}\right)^{n} \cdot \underline{r}_{0} = C_a \cdot \mathrm{I}_{a}^{n} \cdot \underline{r}_{a} + C_b \cdot \mathrm{I}_{b}^{n} \cdot \underline{r}_{b} \tag{5.13b}$$

At this point, in order to derive the stability criteria, it is sufficient to discuss two special cases:

Case A) $\boxed{0 \le g_1 \cdot g_2 \le 1}$

With this condition on the resonator parameters, the radicand in equation (5.12 c) is negative and, thus, the root is imaginary. Using a supporting variable Θ:

$$\Theta = \arccos\left(2 \cdot g_1 \cdot g_2 - 1\right) \tag{5.14a}$$

we can re-write the eigenvalues $\lambda_{a,b}$ as:

$$\lambda_{a,b} = \cos\Theta \pm \sqrt{\cos^2\Theta - 1} = \cos\Theta \pm i \cdot \sin\Theta = \exp(\pm i \cdot \Theta) \qquad (5.14b)$$

Therefore, the ray vector after *n* passes becomes:

$$\underline{r}_n = C_a \cdot e^{in\Theta} \cdot \underline{r}_a + C_b \cdot e^{-in\Theta} \cdot \underline{r}_b$$

It is very important to note that since $\left|e^{\pm in\Theta}\right| = 1$, the absolute value of the ray vector is finite even after infinite number of passes/round-trips. This means that both the distance of the beam to the optical axis and its propagation slope also have finite values.

Case B) $\boxed{g_1 \cdot g_2 < 0 \quad or \quad g_1 \cdot g_2 > 1}$

Assuming these conditions on the resonator parameters, the radicand in (5.12 c) is positive and, hence, the eigenvalues are real:

$$g_1 \cdot g_2 < 0 \quad \Rightarrow \quad \lambda_b < -1$$
$$g_1 \cdot g_2 > 1 \quad \Rightarrow \quad \lambda_a > 1$$

This means that in these conditions the absolute value of one of the eigenvalues is always larger than 1. Thus, the absolute value of the ray vector r_n (i.e. after n passes/round-trips) will grow unbounded for most of the starting vectors. Physically this means that most of the rays expand to the edges of the mirrors and, consequently, experience high losses.

In the context of lasers, usually the most interesting case are resonators fulfilling:

$$0 \le g_1 \cdot g_2 \le 1,$$

which are referred to as <u>stable resonators</u>. In stable resonators the optical rays propagate around/close to the optical axis. All other mirror arrangements not fulfilling this condition are instable resonators. With this information the so-called stability diagram for passive laser resonators can be drawn.

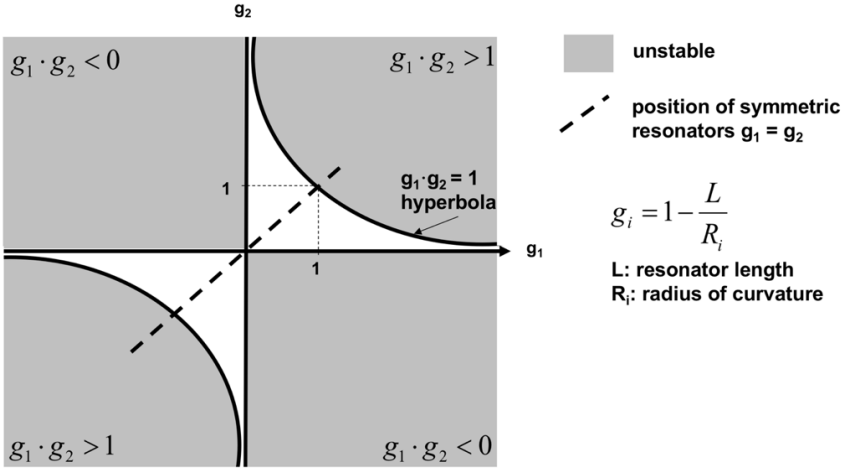

In the stability diagram the dashed line represents symmetric resonators (i.e. those where $g_1 = g_2$). The most important representative of symmetric resonators are the plane-parallel, the confocal and the concentric resonators, which are illustrated below.

A) *Plane-parallel resonator*: $g_1 = g_2 = 1$ (it is located at the edge of the stability region)

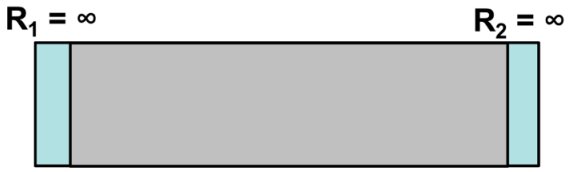

B) mirrors with large radii

C) *Confocal resonator*: $g_1 = g_2 = 0$

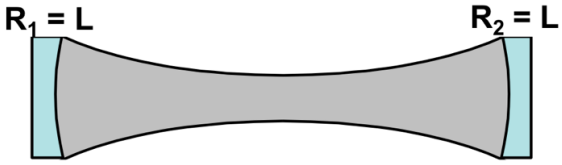

D) *Concentric resonator*: $g_1 = g_2 = -1$ (it is also at the edge of stability)

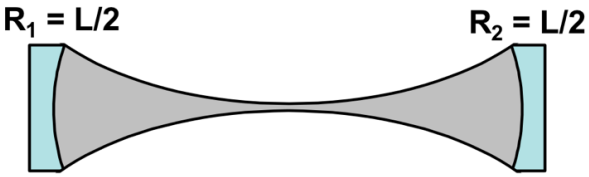

It is worth mentioning that the concentric resonator creates the smallest waist (and, therefore, the highest intensity) among all stable resonators. That feature is very helpful to achieve laser oscillation at transitions characterized by a high pump threshold. It is also worth pointing out that a resonator may also become instable if the curvature of the mirrors is too strong (i.e. if $R < L/2$), i.e. if it goes beyond the concentric point in the stability diagram.

A prominent example for non-symmetric resonators is the hemi-spherical resonator illustrated below.

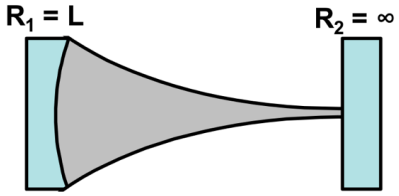

Instable resonators

As discussed above, instable resonators fulfill:

$$g_1 \cdot g_2 < 0 \quad or \quad g_1 \cdot g_2 > 1.$$

Most of the optical rays in such configurations do not remain close to the optical axis after several round-trips. Therefore, the light experiences large propagation losses in these resonators. In spite of this, instable resonators can be advantageous because the radiation pattern within them is typically not concentrated in small volumes but, on the contrary, it is rather large and homogeneous. This can be beneficial to extract the inversion in gain media with large dimensions.

One important example is the confocal instable resonator, which delivers a nearly collimated output beam.

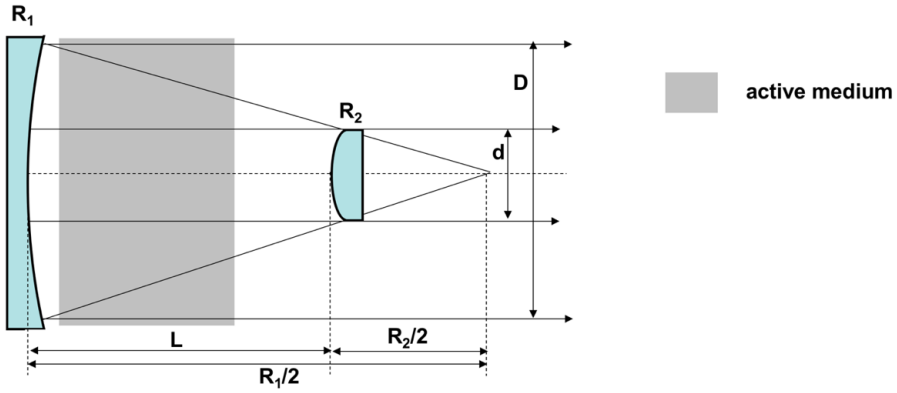

In this kind of resonator the diameter of the active medium should be approximately equal to the diameter of intensity distribution (D). Therefore, the active medium is typically placed close to the mirror with radius of curvature R_1.

The transmission of the "out-coupling mirror" (that of diameter d and radius of curvature $R_2 < 0$) is determined by a geometric area ratio:

$$T_g = 1 - \frac{d^2}{D^2}$$

This kind of unstable resonators find widespread use in high-power CO_2 lasers, excimer lasers and a few solid-state laser setups.

Thermo-optical problems – Thermal Lensing

The laser process generates heat in the active medium which, in most cases, has detrimental consequences to the laser process. On one hand, the beam quality might degrade and, on the other hand, the efficiency might drop. The reason for the heat-load can be found in all non-radiative transitions in the medium.

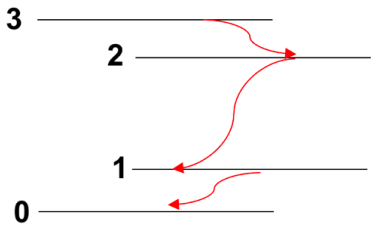

Most of these non-radiative transitions are related to the quantum defect, which was defined as:

$$1 - \frac{n_{21}}{n_{03}}.$$

The difference between the frequency (and therefore energy) of the signal and pump photons is the most obvious source of heat-load in the medium. In addition, the quantum efficiency (between level 2 and level 1) might be smaller than 1 and, therefore, there can also be non-radiative transitions associated with this, which also cause heat. Furthermore, absorption in the host material itself (not in the dopants), also causes heat-load. It is worth mentioning, though, that the use of diode laser pumps instead of flash-lamp pumps can significantly reduce the thermal load caused by absorption and, therewith, the thermo-optical problems as well.

In the following we consider a cylindrical rod as the shape of the active medium (length L, radius r_0).

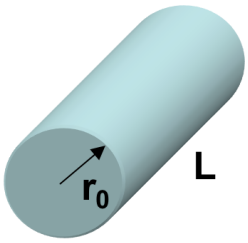

Furthermore, we consider a homogeneous (i.e. position independent) pumping process, which, we assume, causes a homogeneously distributed heat-load (please note that this is not always the case). Cooling occurs along the surface of the cylinder resulting in a strictly radial heat flow. This motivates the use of the one-dimensional heat-conduction equation to describe the temperature profile within the active medium:

$$\frac{d^2T}{dr^2} + \left(\frac{1}{r}\right) \cdot \frac{dT}{dr} + \frac{P_T}{V \cdot K} = 0,$$

where P_T represents the generated heat (source term) and K is the thermal conductivity. The solution in steady-state (i.e. when the thermal load equals the dissipated heat) is given by:

$$T(r) = T(r_0) + \left(\frac{P_T}{4 \cdot V \cdot K}\right)\left(r_0^2 - r^2\right),$$

with $T(r_0)$ being the surface temperature. This equation reveals a parabolic temperature profile inside of the active medium. Using it, we can extract the temperature difference between the center and the surface of the active medium as:

$$T(0) - T(r_0) = \frac{P_T}{4\pi \cdot L \cdot K} \neq f\left(T(r_0)\right),$$

which is independent of the surface temperature.

On top of that, heat dissipation causes a difference between the surface temperature and the temperature of the coolant. This difference in steady-state is given by:

$$T(r_0) - T_C = \frac{P_T}{A_C \cdot h}$$

where T_C is the coolant temperature, A_C is the surface area of the cylinder ($2\pi r_0 \cdot L$) and h is the surface heat-transfer coefficient (taking into account the coolant medium, e.g. air or water, its flow speed, etc.).

Consequently, the temperature in a laser rod has the profile shown in the following figure:

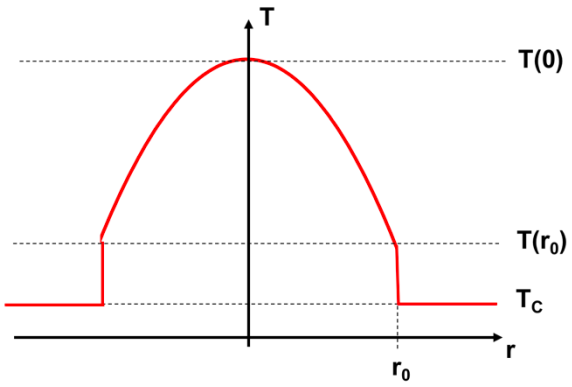

As can be seen, the temperature is characterized by a parabolic profile in the rod and a temperature jump at its surface. It is worth emphasizing that the inner temperature gradient cannot be influenced by the coolant temperature!

The inner gradient is the reason for thermal lensing as it causes a deformation of the end facets due to thermal expansion, a temperature-dependent change of the refractive index and an index change due to the photo-elastic effect. These three temperature-driven effects are discussed in more detail below.

A) end facet deformation

The higher temperature in center of the rod leads to the surfaces bulging. This effectively turns the rod into a thick lens. However, in solids there is no free expansion of the material and stress is induced. As a matter of fact, the curvature only occurs at the edges of the rod and can usually be neglected.

B) gradient of refractive index

The refractive index of a material is temperature-dependent. Therefore, the refractive index in the active medium becomes position-dependent as soon as there is a temperature gradient in the material. In a first order approximation the refractive index can be written as:

$$\Delta n(r) = n(r) - n(0) = \frac{dn}{dT} \cdot [T(r) - T(0)] = -\frac{P_T}{4 \cdot V \cdot K} \cdot \frac{dn}{dT} \cdot r^2$$

where *n(0)* is the refractive index at the center of the rod and *dn/dT* is the thermo-optic coefficient of the material. As a result of the (assumed) homogeneous thermal-load, the index profile has a parabolic shape.

C) photo-elastic effect

The higher temperature in the center of the rod makes it expand against the cooler outer layers of the rod. This results in stress in the medium in both the radial and tangential directions.

The change of refractive index due to the photo-elastic effect in the radial and tangential directions is:

$$\Delta n_r = -\frac{1}{2} \cdot n(0)^3 \cdot \frac{\alpha \cdot P_T}{V \cdot K} \cdot C_r \cdot r^2$$

$$\Delta n_\varphi = -\frac{1}{2} \cdot n(0)^3 \cdot \frac{\alpha \cdot P_T}{V \cdot K} \cdot C_\varphi \cdot r^2$$

with $C_{r,\phi}$ representing the elasto-optical coefficients and α the expansion coefficient.

The difference in elasto-optical coefficients in both directions causes a birefringence, which can be revealed by a stress analysis of a pumped laser crystal (rod) as shown in the figure below.

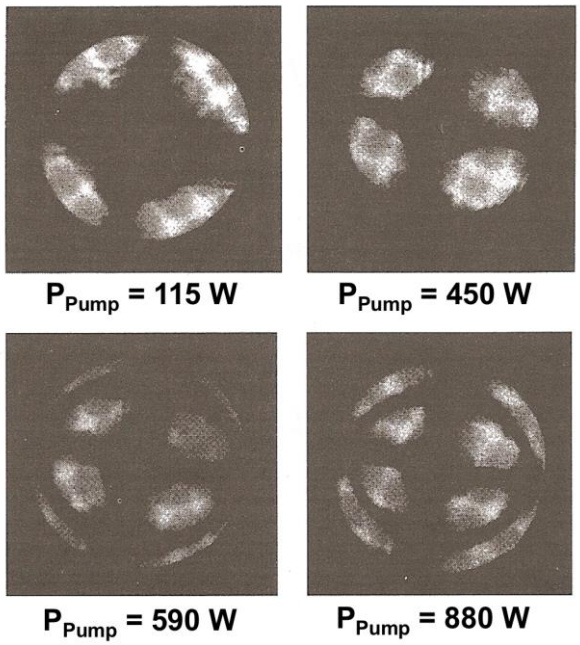

The two essential contributions to the change of the refractive index (i.e. the thermo-optic and the elasto-optic effect) can be summarized in one expression:

$$n(r) = n(0) \cdot \left(1 - \frac{P_T}{2 \cdot V \cdot K} \left(\frac{1}{2 \cdot n(0)} \cdot \frac{dn}{dT} + n(0)^2 \cdot \mathrm{a} \cdot C_{r,\mathrm{j}} \right) \cdot r^2 \right)$$

The quadratic spatial phase variation corresponds to the phase contribution of a spherical lens.

The refractive index profile above can be expressed as:

$$n(r) = n(0) \cdot \left(1 - \frac{2 \cdot r^2}{b^2} \right)$$

,

which corresponds to a lens with the focal length:

$$f \; @ \frac{b^2}{4 \cdot n(0) \cdot L}$$

.

Therefore, the focal length of the thermal lens is given by:

$$f \; @ \frac{K \cdot V}{P_T \cdot L} \left(\frac{1}{2} \frac{dn}{dT} + n(0)^3 \cdot \mathrm{a} \cdot C_{r,\mathrm{j}} \right)^{-1}$$

.

This is a power-dependent focal lens and a power dependent birefringence. Most often this thermal lens causes a degradation of the quality of the emitted laser beam.

5.2 Wave Optical Consideration of Laser Resonators

The stability criteria of passive laser resonators have been derived by means of a ray-optic consideration. Such treatment, however, provides no information about resonance conditions and diffraction losses. A wave-optic consideration is needed to analyze these characteristics.

A common approach in electro-magnetic wave theory is the identification of eigen-oscillations of different structures. In that theory, the ideal case is represented by a spatial area surrounded by perfectly conductive walls. It can be shown that such a configuration does not support DC fields but fields with steady-state oscillations at certain resonance frequencies can exist within this structure. Mathematically these oscillations are solutions of the wave equation under the given boundary conditions (i.e. that the tangential component of the E-field = 0).

In reality, though, the walls are not perfectly conductive and, hence, losses will appear. These, in turn, lead to the mentioned oscillating fields being damped. Strictly speaking, these modes (i.e. oscillating fields) are no eigen-oscillations anymore; they are referred to as quasi-modes. This implies that their oscillation frequency is not sharply defined, because the stronger the damping, the broader the resonance curve gets. One way to quantify the broadening of the resonances is by means of a quality factor Q, which is defined as:

$$Q = \frac{\nu}{\delta\nu} \tag{5.16}$$

with ν being the resonance frequency and $\Delta\nu$ being the bandwidth (FWHM) of the resonance curve.

In a resonator with damping no stationary (i.e. temporally sustained) oscillation can be observed (as it will die off with time). However, if an amplifying (loss compensating) element is introduced into such resonator, oscillation on one or more eigen-frequencies becomes feasible. That is exactly the definition of a laser we already know.

From electro-magnetism theory, it is known that the eigen-frequencies of a cuboid with side lengths *a*, *b*, *c* are given by:

$$\nu_i = \left(\frac{c}{2}\right) \cdot \sqrt{\left(\frac{n_x}{a}\right)^2 + \left(\frac{n_y}{b}\right)^2 + \left(\frac{n_z}{c}\right)^2} \tag{5.17}$$

Where n_x, n_y, n_z are natural numbers (later on, they will be referred to as the mode order). Assuming that *x* is a distinguished resonator direction (e.g. the propagation direction of light), then the value of n_x denotes the order of a longitudinal mode, whereas the values of n_y and n_z denote the order of a transverse mode. The transverse mode with $n_y = 0$ and $n_z = 0$ is referred to as the fundamental mode of the cavity.

In vacuum the oscillation wavelengths of the fundamental mode in a cuboid is given by:

$$\lambda_n = \frac{c}{\nu_n} = \frac{2a}{n_x}$$

which is a result of the standing-wave condition in the *x*-direction (i.e. the resonator length is a multiple integer of half the wavelength). Assuming that the resonator operates at optical frequencies, the dimensions of the resonator are very large in comparison to the wavelength and, consequently n_x, n_y and n_z are very large numbers.

As it happens, it is difficult to obtain laser emission on a well-defined frequency in a closed resonator. Therefore, open resonators are used in laser physics. The most prominent open resonator is the Fabry-Perot resonator. In this resonator modes propagating along the optical axis experience less damping than modes with propagation components perpendicular to the optical axis (since they will eventually reach the edges of the mirrors and leave the resonator). Such an arrangement allows extracting the emitted radiation energy in one direction (creating what we know as a laser beam).

5.3 Fabry-Perot Resonators with Infinitely Extended Mirrors

We consider the following mirror arrangement: two mirrors facing each other that are aligned perpendicularly to the optical axis (z-direction in this case).

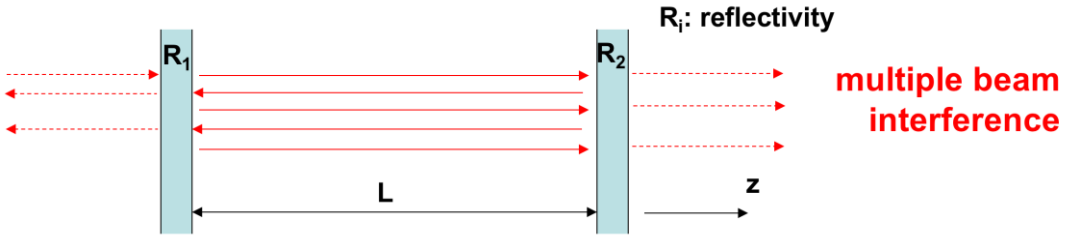

We aim at investigating the influence of cavity losses (i.e. the quality factor) on the resonances and on the transmission characteristics of such a Fabry-Perot resonator. For the time being mirrors with infinite dimensions will be assumed. Therefore, the only source of losses in this resonator are leakage losses through the mirrors.

Now it is assumed that a plane wave propagating in the z-direction illuminates this Fabry-Perot resonator. Thus, a part of it is coupled into this optical arrangement and a certain part is reflected back. To describe the characteristics of the radiation field, we assume that the electric field is linearly polarized in the y-direction. In these circumstances a scalar treatment is sufficient.

Thus, the electric field strength inside the resonator can be written as:

$$E(z,t) = \hat{E}(z) \cdot \cos(\omega \cdot t - \phi) = \mathrm{Re}\left\{ u(z) \cdot \exp(i\omega t) \right\}$$

with

$$u(z) = \hat{E}(z) \cdot \exp(-i \cdot \phi)$$

as the complex amplitude.

One round-trip causes a change of the field strength given by:

$$R = \sqrt{R_1 \cdot R_2}\ ,$$

and a phase-shift of:

$$\omega \cdot \tau_R + 2\pi$$

where τ_R is the cavity round-trip time (=2L/c).

Using the well-known expression of the angular frequency, we can write:

$$\omega \cdot \tau_R = \left(\frac{2\pi c}{\lambda}\right) \cdot \left(\frac{2L}{c}\right) = 4\pi \frac{L}{\lambda} = 2\delta \qquad \text{i.e.} \qquad \delta = 2\pi \frac{L}{\lambda}$$

Using this definition of the phase-shift δ, the change of the complex amplitude after each round-trip is given by:

$$u_n(z) = R \cdot \exp(2 \cdot i \cdot \delta) \cdot u_{n-1}(z)\ .$$

The total complex amplitude is the superposition of all waves inside the resonator, i.e.

$$\begin{aligned} u_{\text{int}} &= u_1 + u_2 + u_3 + u_4 + \ldots \\ &= u_1 \cdot \left\{1 + R \cdot \exp(2 \cdot i \cdot \delta) + R^2 \cdot \exp(4 \cdot i \cdot \delta) + \ldots\right\} \end{aligned}$$

if R<1 such a geometric series converges to

$$u_{\text{int}} = \frac{u_1}{1 - R \cdot \exp(2 \cdot i \cdot \delta)}\ .$$

The absolute value of that complex amplitude reaches its maximum if δ is a multiple integer of π, resulting in:

$$u_{\text{int,max}} = \frac{u_1}{1 - R}$$

The maximum of the absolute value of the complex amplitude occurs if the cavity length and resonance frequency fulfill the following conditions:

$$n \cdot \frac{\lambda}{2} = L \quad \text{and} \quad \nu = n \cdot \frac{c}{2L} \tag{5.18a}$$

Hence, in the spectrum it is possible to observe equally spaced resonance frequencies. Their separation is called the free spectral range (FSR), which is determined by:

$$\Delta\nu = \frac{c}{2L} = \frac{1}{\tau_R} \ . \tag{5.18b}$$

Additionally, the intensity inside the Fabry-Perot cavity is proportional to:

$$\left|u_{\text{int}}\right|^2 = u_{\text{int}} \cdot u_{\text{int}}^* \ ,$$

which allows obtaining the ratio between the transmitted intensity and the intensity at a resonance as a function of the phase shift in the cavity (sometimes referred to as Airy function):

$$\frac{I}{I_{\max}} = \frac{(1-R)^2}{(1-R\cdot\exp(2\cdot i\cdot\delta))\cdot(1-R\cdot\exp(-2\cdot i\cdot\delta))} = \frac{1}{1+\dfrac{4\cdot R\cdot\sin^2\delta}{(1-R)^2}} \tag{5.19a}$$

Plotting this function for two values of the mirror reflectivity R, we can conclude that a higher R (lower losses) leads to narrower resonances.

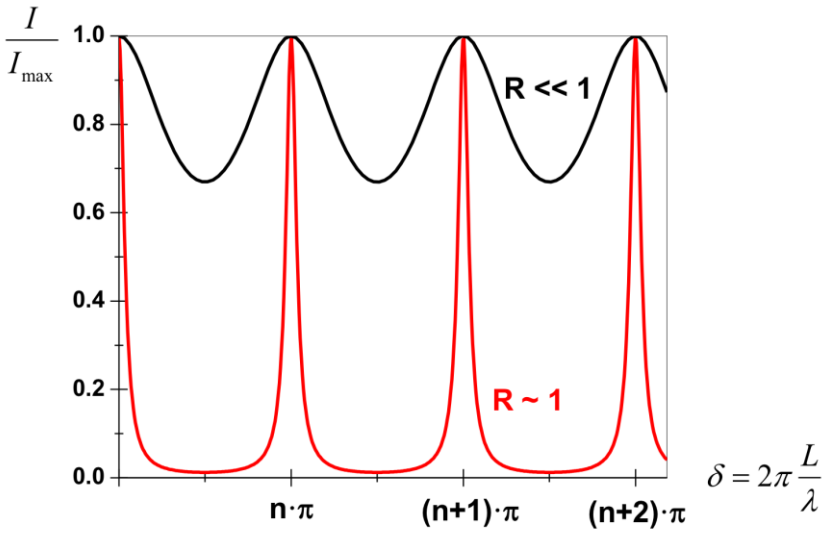

For small deviation of the phase-shift from the resonance, we can approximate the sin-function in equation (5.19a) by:

$$\sin^2\delta = \sin^2(n\pi - \delta) \approx (n\pi - \delta)^2$$

Now it is possible to re-write the ratio of the transmitted intensity to the intensity at a resonance using this approximation as:

$$\frac{I}{I_{\max}} = \frac{\Gamma^2/4}{(n\pi - \delta)^2 + \Gamma^2/4}$$

with

$$\Gamma^2 = \frac{(1-R)^2}{R} \quad . \tag{5.19b}$$

This reveals that, close to the resonance, the function I/I_{max} can be approximated by a Lorentz profile with a half width (FWHM) Γ.

An important parameter to describe the characteristics of a cavity is the finesse F, which is defined as:

$$F = \frac{FSR}{\Gamma} = \frac{\pi}{\Gamma} = \frac{\pi\sqrt{R}}{1-R} \quad . \tag{5.20}$$

Thus, using equation (5.18b), the FWHM linewidth of the resonance in the frequency domain becomes:

$$\Gamma = \frac{FSR}{F} \Rightarrow \delta\nu_R = \frac{\Delta\nu}{F} = \frac{1}{F \cdot \tau_R}$$

It is worth mentioning that this bandwidth corresponds to the transmission characteristics of the Fabry-Perot resonator and not to the actual emission bandwidth of a laser operating at one of the longitudinal modes.

5.4 Fabry-Perot Resonators with Finite Mirror Dimensions

In the following section we will investigate the influence of mirror clipping effects on characteristics of the resonance (derived in section 5.3).

To do so, the resonator is replaced by an infinite series of lenses which are separated by a distance which is a multiple of half the signal wavelength. Such an arrangement is known as lens-guide. In the case of a plane-parallel Fabry-Perot resonator these lenses have an infinite focal length (i.e. they will be flat and, can, therefore, be replaced by free-space). The finite mirror dimensions are simulated by apertures.

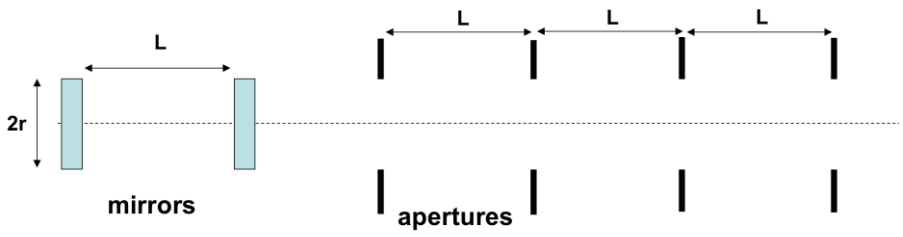

To further simplify the situation, we assume that the mirrors are just limited in one dimension. Hence, the lens-guide is a series of infinitely long slits of finite width. If a plane wave illuminates the first aperture, a diffraction pattern will evolve after it, namely the diffraction of an infinitely long slit.

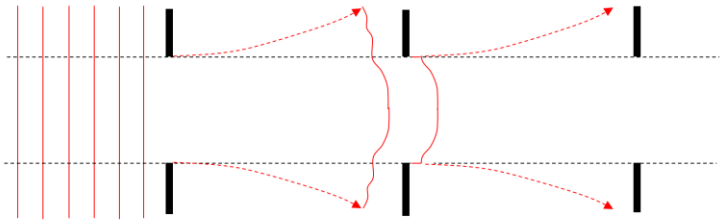

The diffraction pattern itself can be calculated using Kirchhoff's integral within the scope of near-field (Fresnel) diffraction. From that, it is known that the shape of the diffraction pattern is determined by the slit dimensions and by the wavelength of light. Obviously, due to diffraction in the first slit, the 2nd slit is not illuminated by a plane wave any more. In particular perturbations at the edges and a slight divergence can be observed. All subsequent slits are also not illuminated by a plane wave. Therefore, numerical methods are required to describe the light propagation through such a series of apertures. These numerical simulations reveal that after a large number of passes (>100) through the apertures, stable field distributions develop. Further passes do not alter the shape, but only lead to a loss of power (truncation loss). It is noteworthy that the losses of the stable field distribution are significantly lower than the losses experienced by the field as it went through the first slits. That observation justifies considering the stable field distribution as an eigen-mode of the optical arrangement.

Finally, we can fold back the series of apertures to a resonator. In this analogy it can be seen that the diffraction losses (clipping on the mirrors) should act in the same way as the transmission losses (leakage through the mirror): They reduce the Q factor and, therewith, broaden the resonances.

It can be shown that the stable field distribution is nearly independent of the wavelength, i.e. different longitudinal modes possess the same spatial distribution and, therefore, the obtained stable distribution constitutes a transverse fundamental mode, which has been achieved by starting with a plane wave. Higher-order transverse modes can be obtained by starting with different field distributions such as:

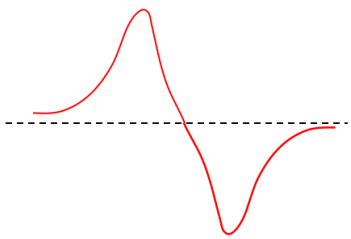

The details of higher-order transverse modes will be described later in the script. For the moment it is sufficient to learn that higher-order transverse modes have more intricate intensity patterns and are characterized by higher diffraction losses.

The relations in the resonator do not change if the resonator dimension and wavelength are scaled by the same factor. Therefore, it can be beneficial to introduce a quantity that is invariant to such a scaling. Such a quantity is the Fresnel number N_F, defined as:

$$N_F = \frac{r^2}{\lambda \cdot L} \tag{5.22}$$

Where r is the transversal dimension of the resonator (in case of circular mirrors, for example, *r* is the radius of the mirrors). The Fresnel number is basically the ratio between the acceptance angle and the diffraction angle. Hence, the smaller the N_F, the higher the diffraction losses are.

The following figure illustrates the diffraction losses per round-trip for different transverse modes in a resonator with circular mirrors. TEM stands for transverse electro-magnetic wave and the subscripts describe the mode order (00 being the fundamental mode, while the others are higher-order modes).

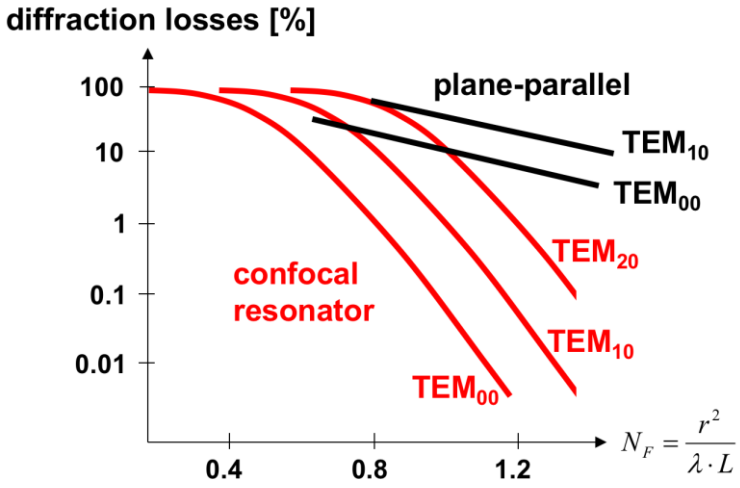

The confocal resonator is characterized by the smallest mode radii on mirrors amongst all resonator configurations (for given resonator dimensions). Therefore, light in the confocal resonator experiences the lowest diffraction losses for any given Fresnel number.

In the case of the plane-parallel resonator (with $R_1 = R_2$ = infinity), the mode radii at the mirrors tend to infinity and, thus, high diffraction losses can be expected.

Again, higher-order transverse modes have higher losses, a property which is exploited for mode selection within a resonator.

5.5 Gaussian beams and the Fundamental Mode in Stable Resonators

In the previous section we have learned that the intra-cavity field distribution does not correspond to that of a simple plane wave. Of course, the field distribution has to be a solution of the wave-equation with a radially decaying intensity; whereby the well-known wave-equation is given by:

$$\Delta\vec{E} = \frac{1}{c^2}\frac{\partial^2\vec{E}}{\partial t^2} \quad .$$

We restrict the consideration to monochromatic fields and to a scalar treatment. Hence, the ansatz

$$E(x,y,z,t) = u(x,y,z)\cdot\exp(i\omega t)$$

leads to the time-independent scalar wave-equation (also known as Helmholtz equation):

$$\Delta u + k^2 u = 0$$

with

$$k = \frac{\omega}{c} = \frac{2\pi}{\lambda}$$

as the absolute value of the wave vector. Furthermore, we assume that the light beam propagates in the *z*-direction and that its characteristics of propagation do not differ too much from those of a plane wave. That allows using the following ansatz for *u*:

$$u(x,y,z) = \Psi(x,y,z)\cdot\exp(-ikz)$$

where

$$\exp(-ikz)$$

is a plane wave propagating in the *z*-direction and

$$\Psi(x,y,z)$$

indicates a deviation from an ideal plane wave.

In addition, we assume a weak *z*-dependence of that function of deviation from the plane wave (Ψ), what can be expressed as:

$$\left|\frac{\partial^2\Psi}{\partial z^2}\right| << \left|k\cdot\frac{\partial\Psi}{\partial z}\right|$$

leading to the paraxial Helmholtz equation:

$$\frac{\partial^2\Psi}{\partial x^2}+\frac{\partial^2\Psi}{\partial y^2}-2ik\frac{\partial\Psi}{\partial z}=0 \ .$$

The problem can be simplified by performing a conversion to cylindrical coordinates, i.e.

$$r^2=x^2+y^2 \ .$$

The solution of the paraxial Helmholtz equation can be then calculated with the ansatz:

$$\Psi=\Psi_0\cdot\exp\left\{-i\left(p(z)+\frac{k\cdot r^2}{2\cdot q(z)}\right)\right\} \qquad \text{(5.23 a)}$$

where *p* is the *complex phase-shift* and *q* is the *complex beam parameter*.

By introducing equation (5.23 a) in the paraxial Helmholtz equation (in cylindrical coordinates) it is possible to derive the two differential equations to determine the functions *p* and *q*:

$$\frac{dp}{dz}=-\frac{i}{q(z)}$$

$$\frac{dq}{dz}=1 \qquad \text{(5.23 b and c)}$$

The simple integration of equation (5.23 c) results in the following evolution of *q* with *z*:

$$q(z_2)=q(z_1)+(z_2-z_1) \ . \qquad \text{(5.24a)}$$

In order to gain some insight in the propagation characteristics of the field distribution, we can express *q* as a function of physically relevant quantities, i.e. the beam radius (*w*) and the radius of curvature of the phase-front (*R*), as:

$$\frac{1}{q(z)}=\frac{1}{R(z)}-i\frac{\lambda}{\pi\cdot w(z)^2} \ . \qquad \text{(5.24b)}$$

By inserting equation (5.24 b) in the ansatz for the deviation from the plane wave (Ψ), i.e. equation (5.23 a), we can write:

$$\Psi=\Psi_0\cdot\exp\{-i\cdot p(z)\}\cdot\exp\left\{-i\frac{k\cdot r^2}{2\cdot R(z)}\right\}\cdot\exp\left\{-\frac{r^2}{w(z)^2}\right\} \qquad \text{(5.25a)}$$

Besides having an amplitude Ψ_0, it is possible to see that the function Ψ exhibits a z-dependent deviation from the phase of a plane wave, an r-dependent phase-factor and a radially decaying amplitude (that corresponds to a Gaussian function).

Assuming at position $z = 0$ a given field distribution with a plane phase-front (i.e. $R(0)=\infty$), the field distribution is given by a Gaussian function:

$$\Psi = \Psi_0 \cdot \exp\left\{-\frac{r^2}{w_0^2}\right\},$$

with w_0 being the beam radius at position z=0 (i.e. at focus / at the beam waist). This means that, at a radius r=w_0 from the optical axis, the amplitude of the field is a factor 1/e smaller than the peak value on the optical axis (i.e. r=0).

At $z = 0$ the radius of curvature of the wavefront is infinite. Hence, the beam parameter q becomes purely imaginary (see 5.24 b):

$$q(0) = q_0 = i\frac{\pi \cdot w_0^2}{\lambda} = i \cdot z_R .$$

In this last expression the definition of the Rayleigh length z_R is

$$z_R = \frac{\pi \cdot w_o^2}{\lambda}$$

Using equation (5.24 a) it is possible to rewrite the evolution of q in the following form:

$$q(z) = q_0 + z = i \cdot z_R + z . \qquad (5.25.b)$$

The comparison between the real and imaginary parts of equations (5.25 b) and (5.24 b) provides an expression for the evolution of the beam radius $w(z)$:

$$w(z) = w_0 \cdot \sqrt{1+\left(\frac{z}{z_R}\right)^2} , \qquad (5.25\ c)$$

and the radius of curvature of the phase-front $R(z)$:

$$R(z) = z + \frac{z_R^2}{z} . \qquad (5.25\ d)$$

The following figure illustrates the evolution of the beam radius as a function of the distance (in the z-direction) from the beam waist.

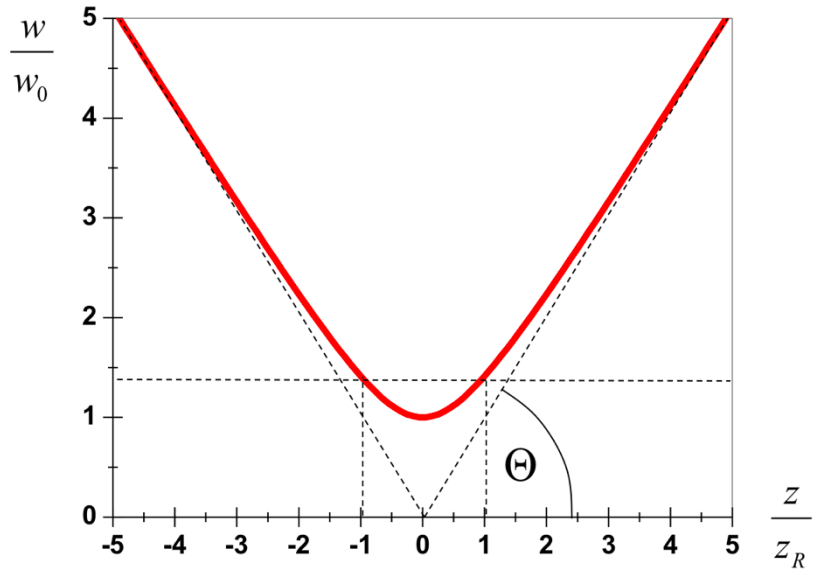

The beam radius w reaches its minimum at $z = 0$ (waist). In the proximity of the waist (i.e. when $z < z_R$) the beam radius changes just slowly. In fact, within the Rayleigh range (i.e. $-z_R \le z \le z_R$) the beam is considered collimated.

At exactly the position of the Rayleigh length, the beam radius is a factor $\sqrt{2}$ larger than at the focus:

$$z = \pm z_R \quad \Rightarrow \quad w(\pm z_R) = \sqrt{2} w_0$$

and for large distances away from the focus, the beam size increases approximately linearly with the distance z:

$$w(z) \approx w_0 \cdot \frac{z}{z_R} \qquad (5.25\ c)$$

Consequently, the beam expands almost with a constant aperture angle Θ (for $|z| >> z_R$):

$$\Theta = \arctan\left(\frac{w(z)}{z}\right) \approx \arctan\left(\frac{w_0}{z_R}\right) = \arctan\left(\frac{\lambda}{\pi \cdot w_0}\right) \quad \text{i.e.} \quad \Theta \cdot w_0 \approx const.$$

According to the expression above, the larger the beam radius in the waist the smaller this aperture angle will be. Thus, the divergence of a Gaussian beam can be considered as a diffraction effect, i.e. a consequence of the limited beam diameter at the waist.

The radius of curvature of the wave-front as a function of the distance from the beam waist is shown in the plot below.

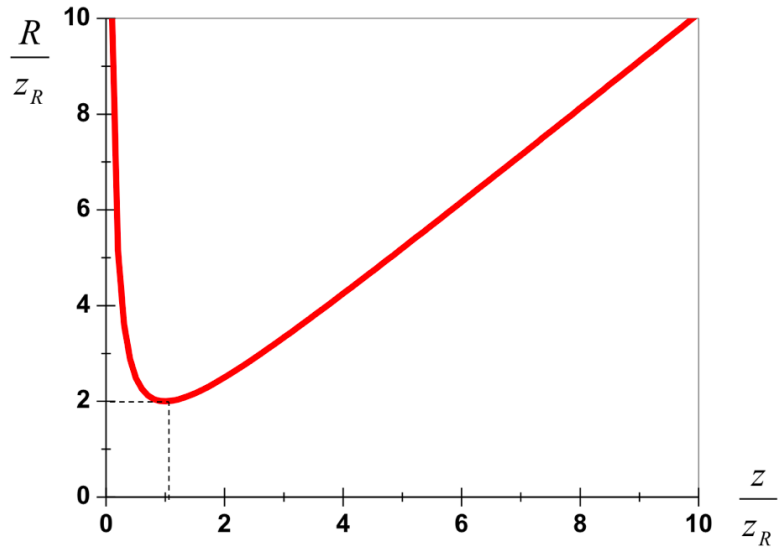

As defined earlier, the radius of curvature is infinity at the waist position, that is $R(z=0)=\infty$, and reaches its minimum at the Rayleigh length:

$$z=\pm z_R \quad \Rightarrow \quad R(\pm z_R)=2\cdot z_R \,,$$

before increasing linearly for large distances *z* from the waist (from (5.25 d)):

$$z>>z_R \quad \Rightarrow \quad R(z)\approx z \,.$$

This behavior corresponds to the wavefront of a spherical wave starting at the origin.

When inserting equation (5.25 b) in (5.23 b) it is possible to derive the complex phase shift *p(z)* by considering:

$$\frac{dp}{dz}=-\frac{i}{q(z)}=-\frac{i}{z+i\cdot z_R}\,.$$

That differential equation has the solution:

$$p=-i\cdot\ln\left(1-i\frac{z}{z_R}\right)=-i\cdot\ln\sqrt{1+\left(\frac{z}{z_R}\right)^2}-\arctan\left(\frac{z}{z_R}\right)$$

Therewith, using equation. (5.25 c), the complex phase-shift contributes to Ψ through:

$$\exp\{-i\cdot p(z)\}=\frac{w_0}{w(z)}\exp\{i\cdot\Phi(z)\}$$

i.e. it leads to a reduction of the amplitude with propagation and to a deviation from the phase of a plane wave according to:

$$\Phi(z) = \arctan\left(\frac{z}{z_R}\right),$$

which is known as the *Gouy phase-shift*.

We can use this knowledge about Gaussian beams to calculate the eigenmodes of optical resonators. It is known that, by replacing the wavefront of a beam (i.e. a surface with the same phase) with a mirror, the beam will get reflected, and it will retrace its own path. In addition, some diffraction at the edges of the mirror might occur.

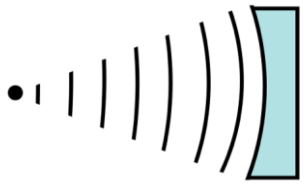

Gaussian beams possess wavefronts that are surfaces of a sphere, i.e. we can use spherical mirrors to achieve the back-reflection of the beam to its own origin.

To construct a resonator, we assume a resonator consisting of two spherical mirrors facing each other and a Gaussian beam bouncing between them. Thus, to each position *z* belongs a particular beam radius *w(z)*:

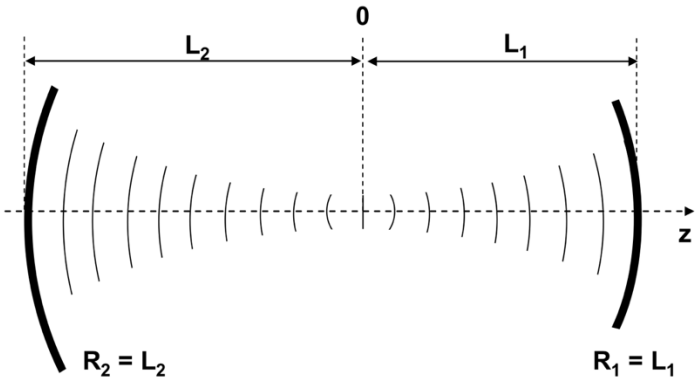

The well-known precondition for an eigenmode is that it should accumulate a phase-shift per round-trip equal to a multiple integer of 2π. For Gaussian beams we need to consider the deviation of the phase from that of a plane wave, i.e. the Gouy-phase. Therefore, for half of a round-trip we can write:

$$n \cdot \pi = \frac{2\pi}{\lambda} \cdot (L_1 + L_2) - \left[\arctan\left(\frac{L_1}{z_R}\right) + \arctan\left(\frac{L_2}{z_R}\right)\right]$$

Consequently, the resonance frequencies are given by:

$$\upsilon = \frac{c}{2L} \cdot \left\{ n + \frac{1}{\pi} \cdot \left[\arctan\left(\frac{L_1}{z_R} \right) + \arctan\left(\frac{L_2}{z_R} \right) \right] \right\}.$$

Using the relation for the cavity length and the definition of the resonator parameters:

$$L = L_1 + L_2 \quad \text{and} \quad g_1 = 1 - \frac{L}{R_1} \qquad g_2 = 1 - \frac{L}{R_2},$$

the resonance frequencies can be rewritten as:

$$\upsilon = \frac{c}{2L} \cdot \left\{ n + \frac{1}{\pi} \cdot \arccos\left(\sqrt{g_1 \cdot g_2} \right) \right\}.$$

The frequency separation between consecutive eigen-frequencies (i.e. the free spectral range (FSR)) is identical to the expression we know from the plane wave consideration:

$$\Delta\upsilon = \frac{c}{2L}$$

So far we have adapted the resonator to a Gaussian beam. However, a more realistic scenario is that 2 mirrors with their radii of curvature and a particular separation (R_1, R_2, L) are given, and we should look for the Gaussian beam which represents the eigenmode of that resonator configuration.

In order to do this, we can use the radius of the wavefront of a Gaussian beam (5.25 d):

$$R(z) = z + \frac{z_R^2}{z}$$

which has to be identical to the radii of curvature of the mirrors at their positions (relative to the beam waist) L_1 and L_2, i.e.

$$R_1 = R(L_1) = L_1 + \frac{z_R^2}{L_1} \quad \text{and} \qquad R_2 = R(L_2) = L_2 + \frac{z_R^2}{L_2} \quad \text{and} \qquad L = L_1 + L_2$$

These three equations can be used to determine the three unknown parameters L_1, L_2 and z_R as:

$$L_1 = g_2 \cdot (1 - g_1) \cdot \frac{L}{G} \qquad (5.27a)$$

$$L_2 = g_1 \cdot (1 - g_2) \cdot \frac{L}{G} \qquad (5.27b)$$

$$z_R^2 = g_1 g_2 \cdot (1 - g_1 g_2) \cdot \frac{L^2}{G^2} \qquad (5.27c)$$

These expressions use the parameter *G* given by:

$$G = g_1 + g_2 - 2g_1g_2 .$$

The only condition for the existence of a solution (according to 5.27 a-c) is that the Rayleigh length is a real quantity, i.e.

$$z_R^2 \geq 0$$

which corresponds exactly with the stability criteria obtained with the ray-optical consideration:

$$0 \leq g_1 \cdot g_2 \leq 1$$

Hence, *stable resonators possess Gaussian beams as their fundamental mode. Conversely, no Gaussian beams can be found as eigenmodes of unstable resonators.*

With equations (5.27 a-c) it is possible to calculate the position of the waist and the Rayleigh length z_R. Moreover using (5.25 c) gives the mode radii on the mirrors. In the following, two examples are provided.

Example 1: L = 30 cm, $R_1 = R_2 = 60$ cm, $\lambda = 1\mu m$

$$g_1 = g_2 = 1 - \frac{L}{R_{1,2}} = \frac{1}{2} \qquad L_2 = L_1 = \frac{L}{2} \qquad G = g_1 + g_2 - 2g_1g_2 = \frac{1}{2}$$

$$z_R = \sqrt{g_1g_2 \cdot (1 - g_1g_2) \cdot \frac{L^2}{G^2}} = \sqrt{\frac{3}{4}} \cdot 0.3\,m = 0.259\,m \qquad w_0 = \sqrt{\frac{z_R \cdot \lambda}{\pi}} = 287\,\mu m$$

$$w(L_1) = w(L_2) = w_0 \cdot \sqrt{1 + \left(\frac{L_1}{z_R}\right)^2} = 332\,\mu m \qquad R(L_1) = R(L_2) = L_1 + \frac{z_R^2}{L_1} = 0.6\,m$$

Example 2: L = 30 cm, $R_1 = R_2 = 16$ cm, $\lambda = 1\mu m$

$$g_1 = g_2 = 1 - \frac{L}{R_{1,2}} = -\frac{7}{8} \qquad L_2 = L_1 = \frac{L}{2} \qquad G = g_1 + g_2 - 2g_1g_2 = -3.281$$

$$z_R = \sqrt{g_1g_2 \cdot (1 - g_1g_2) \cdot \frac{L^2}{G^2}} = 0.0387\,m \qquad w_0 = \sqrt{\frac{z_R \cdot \lambda}{\pi}} = 111\,\mu m$$

$$w(L_1) = w(L_2) = w_0 \cdot \sqrt{1 + \left(\frac{L_1}{z_R}\right)^2} = 444\,\mu m \qquad R(L_1) = R(L_2) = L_1 + \frac{z_R^2}{L_1} = 0.16\,m$$

We know that in a stable resonator configuration the out-coupling occurs via one mirror that is partially transmitting. This does not alter the spatial structure of the beam, but only

leads to a loss of energy, i.e. a part of the Gaussian beam is just coupled out of the cavity. Hence, outside of the cavity the properties of the beam are determined by the position and diameter of the waist in the cavity. Placing an active medium in the resonator, it is possible to realize a laser oscillator which will emit a Gaussian beam above threshold.

Optical Imaging of Gaussian beams

A lens does not change the radius of a beam but its wavefront is deformed through the action of the lens.

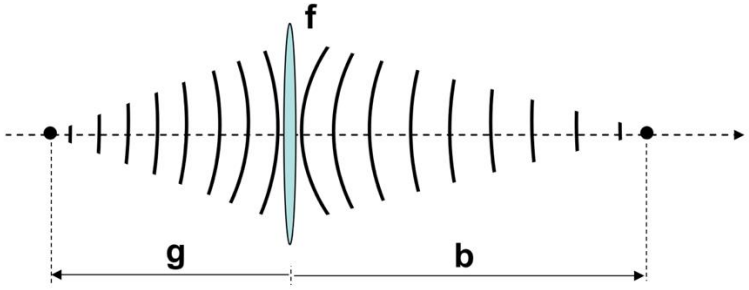

The well-known lens-law describes the relation between the distances *g* and *b* to the focal length *f* of the thin lens (convention: *g* is negative, *b* is positive).

$$\frac{1}{b}-\frac{1}{g}=\frac{1}{f}$$

The radii of curvature of the wavefronts have to fulfil $R_1 = -g$ before the lens and $R_2 = -b$ after the lens, i.e. the lens-law can be re-written as:

$$\frac{1}{R_2}=\frac{1}{R_1}-\frac{1}{f}$$

Taking into account equation (5.24 b), the effect of a thin lens can be described by means of the *q* parameter

$$\frac{1}{q_2}=\frac{1}{q_1}-\frac{1}{f}$$

Thus, the lens creates a beam which is fully characterized by q_2 (which encompasses both the curvature of the wavefront and the beam radius). This knowledge can be used for mode-matching, e.g. for imaging the position and size of the waist into a resonator or into a waveguide.

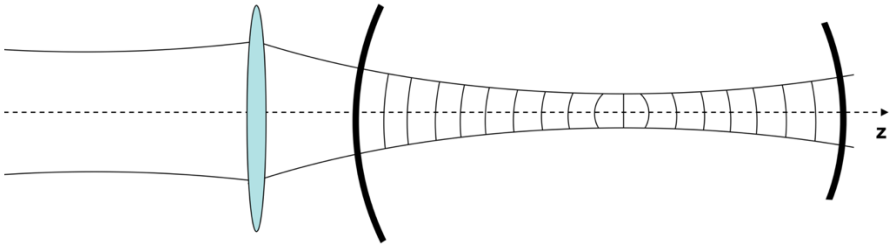

It is important to note that the product of the divergence and the beam radius of a Gaussian beam is conserved through an imaging system. Consequently it is an important parameter that can be used to characterize the laser beam: the so-called *beam parameter product (bpp)*:

$$bpp = \Theta \cdot w_0$$

with Θ being the half-aperture angle [mrad] and w_0 being the beam radius in the waist [mm].

For a Gaussian beam (i.e. for the fundamental mode of a stable resonator) the bpp depends only on the wavelength:

$$\Theta \cdot w_0 \approx \frac{\lambda}{\pi}$$

In practice, however, larger beam parameter products than in the ideal case can be observed, e.g. due to thermo-optical problems in the active medium. For real beams both the divergence (aperture angle) and the beam radius at the waist are usually larger by a factor M than those expected in the ideal case. This can be interpreted as being the result of an incoherent superposition of the fundamental mode and higher-order modes:

$$\Theta = M^2 \cdot \frac{\lambda}{\pi \cdot w_0}$$

The quantity M^2 is the beam quality factor and is a measure of how well a laser beam can be focused.

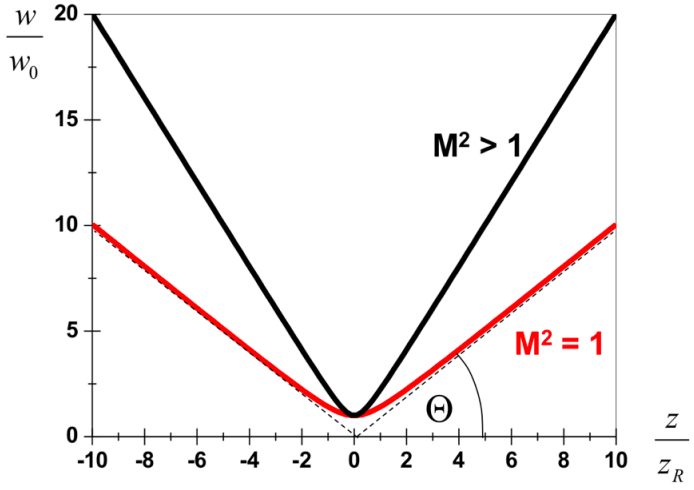

5.6 Higher-Order Transverse Modes in Stable Resonators

In the previous section we have learned that the fundamental mode in a stable resonator is a Gaussian beam, which is often referred to as TEM_{00} (TEM: transverse electro-magnetic wave, 00: lowest transverse mode order). Higher-order transverse modes possess more intricate intensity distributions. However, their field distributions are also solutions of the wave-equation under the given boundary conditions. It is possible to distinguish between rectangular and circular boundary conditions.

Assuming a rectangular geometry, i.e. rectangular mirrors, the intensity distribution of transverse modes including higher order modes (TEM_{mn}) is given by

$$I_{mn}(x,y) \sim H_m^2\left(\frac{x}{w}\right) \cdot H_n^2\left(\frac{y}{w}\right) \cdot \exp\left(-2\left\{\left(\frac{x}{w}\right)^2 + \left(\frac{y}{w}\right)^2\right\}\right)$$

with $H_{m,n}$ being the m/n-th order Hermite polynomial and w being the beam radius.

Examples of such intensity distributions are:

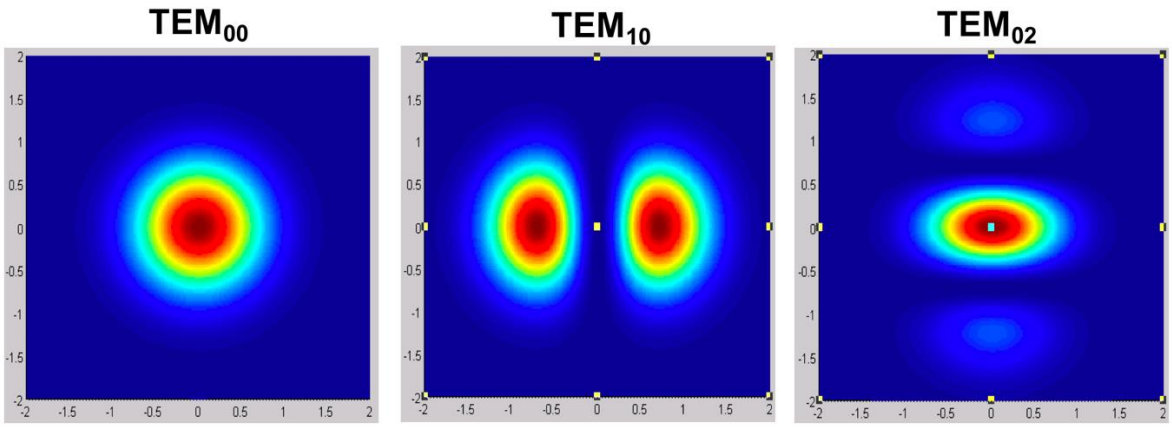

The intensity distribution can be used to identify the mode order as the number of zero points in the horizontal and vertical directions are equal to m and n, respectively.

Assuming a circular geometry (mirrors) the modal intensity distribution can be written as

$$I_{pl}(r,\phi) \sim \left(\frac{2r^2}{w^2}\right)^l L_p^l\left(\frac{2r^2}{w^2}\right) \cdot \cos^2(l\phi) \cdot \exp\left(-\frac{2r^2}{w^2}\right)$$

where L^l_p is the generalized Laguerre polynomial. Examples of intensity distributions are shown in the following figure:

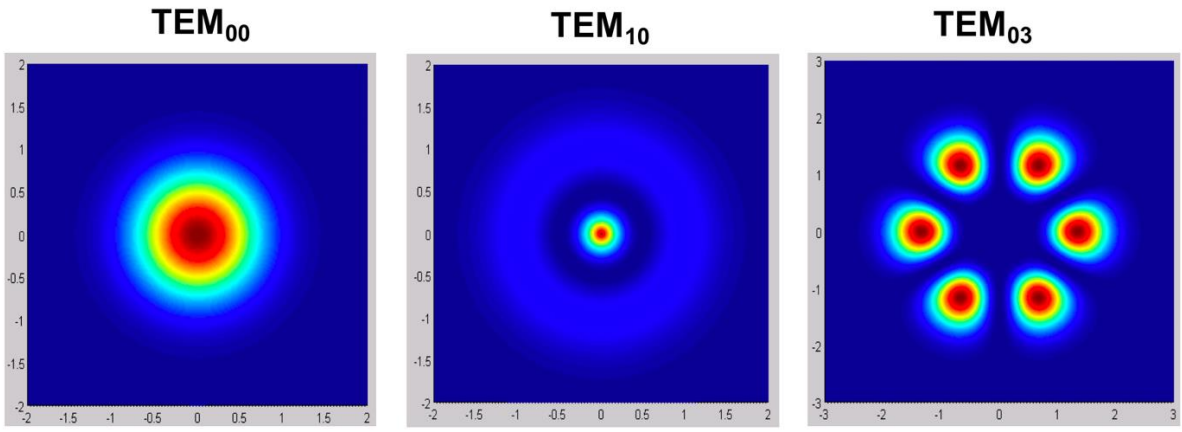

The mode order of the corresponding TEM_{pl} mode (i.e. *p* and *l*) are the number of zero points in the radial and azimuthal directions, respectively.

In both symmetries the TEM_{00} (i.e. the fundamental mode) has a Gaussian profile.

As a matter of fact, the propagation characteristics of higher-order modes differ from those of the fundamental mode. Their beam radius and their divergence increase with increasing mode order (*p,l*) or (*m,n*) according to:

$$w_{pl} = w \cdot \sqrt{2p + l + 1} \qquad w_{x,m} = w \cdot \sqrt{2m+1} \quad w_{y,n} = w \cdot \sqrt{2n+1}$$

$$\Theta_{pl} = \Theta \cdot \sqrt{2p + l + 1} \qquad \Theta_{x,m} = \Theta \cdot \sqrt{2m+1} \quad \Theta_{y,n} = \Theta \cdot \sqrt{2n+1}$$

with *w* representing the TEM_{00} beam radius and Θ being the divergence of the TEM_{00}.

In addition, the different propagation characteristics of higher-order modes lead to a different Gouy-phase shift and, thus, to different eigen-frequencies of modes (*m,n,q*), whereby *q* is the longitudinal mode order:

$$\upsilon_{m,n,q} = \frac{c}{2L} \cdot \left\{ q + \frac{1}{\pi} \cdot (m + n + 1) \cdot \arccos\left(\sqrt{g_1 \cdot g_2} \right) \right\}$$

Considering a plane-parallel resonator (i.e. $g_1 = g_2 = 1$) it is possible to recognize that all transverse modes have the same eigen-frequency:

$$\arccos\left(\sqrt{g_1 \cdot g_2} \right) = 0 \quad \Rightarrow \quad \upsilon_q = \frac{c}{2L} \cdot q$$

On the other hand, in a resonator formed by mirrors with large radii of curvature a so-called mode spectrum can be observed (i.e different transverse modes have different eigen-frequencies).

$$\arccos\left(\sqrt{g_1 \cdot g_2} \right) << 1$$

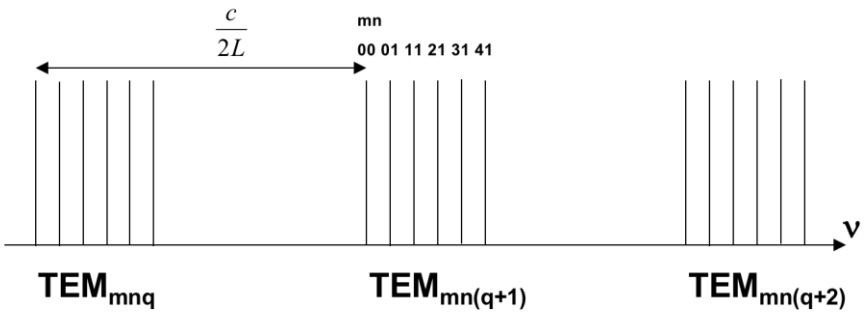

A special case is the confocal resonator ($g_1 = g_2 = 0$). The fact that:

$$\arccos(0) = \frac{p}{2}$$

leads to degenerated eigen-frequencies of different transverse modes:

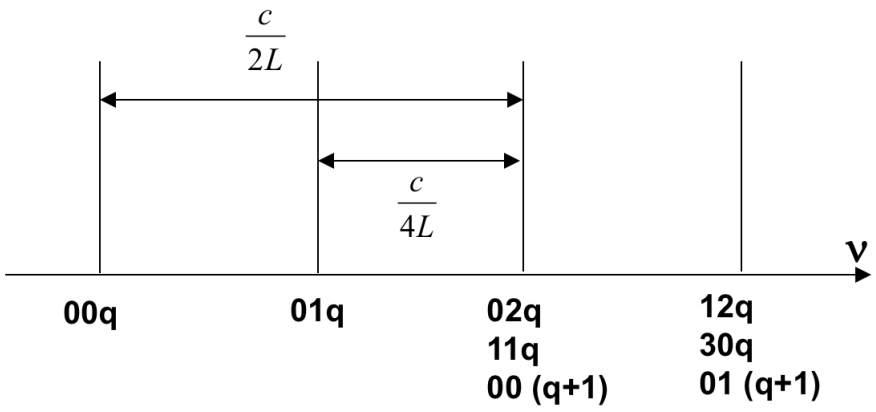

5.7 Selection of Modes

5.7.1 Selection of Transverse Modes

We have just learned that in stable resonators fairly small beam radii of the fundamental mode can be found at the waist (example: L = 1 m, R = 2 m, λ = 1.06 µm => $w_0 \approx 500$ µm). Considering now an inverted area which is larger than the dimensions of the TEM_{00}, higher-order transverse modes might use the inversion which is not extracted by the fundamental mode. In doing so they may even reach their threshold and start to oscillate. The result is an emission which is an incoherent superposition of several transverse modes.

However, many applications rely on fundamental mode beam quality, because the fundamental mode has the lowest possible divergence, it can generate the highest possible power density and its intensity profile is smooth (not structured). Hence, it is worth discussing ways to select transverse modes and, in particular, ways to discriminate higher-order modes.

One possibility is the use of intra-cavity apertures. Such apertures introduce high losses for higher-order modes as they possess larger radial dimensions. Consequently they

experience higher diffraction losses than the fundamental mode and their threshold pump power is increased.

Another possibility to discriminate the higher-order modes is to adapt the resonator design. This way it is possible to increase the dimensions of the TEM_{00} mode to optimize its overlap with the active region.

As an alternative, mode-selective pumping is an also an option, i.e. the matching of the pump spot-size to that of the fundamental mode.

5.7.2 Selection of Longitudinal Modes

Typically, a large number of longitudinal modes are present and might be able to oscillate in a laser. There are several strategies to reduce the number of oscillating frequencies. Independently of the strategy chosen, the precondition for single-frequency emission is the operation of the laser in transverse fundamental mode. The reason is that different transverse modes can have different eigen-frequencies.

In the case of inhomogeneous line broadening light at a certain frequency interacts only with those particles having the right transition frequency (i.e. the interaction takes place only with the right class of particles). Therefore, during laser operation gain saturation happens only on narrow spectral regions around the oscillating longitudinal modes. This effect is known as “spectral hole burning”. In an inhomogeneously broadened active medium emission on multiple longitudinal modes is expected as illustrated below.

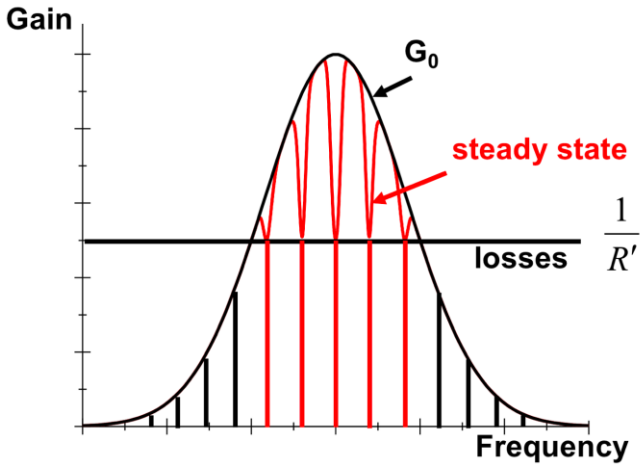

In the case of homogeneous broadening, at the beginning of the laser emission the gain is reduced homogeneously until just one contact point between the gain and the loss line (1/R’) exists, which should result, in principle, in single longitudinal-mode operation.

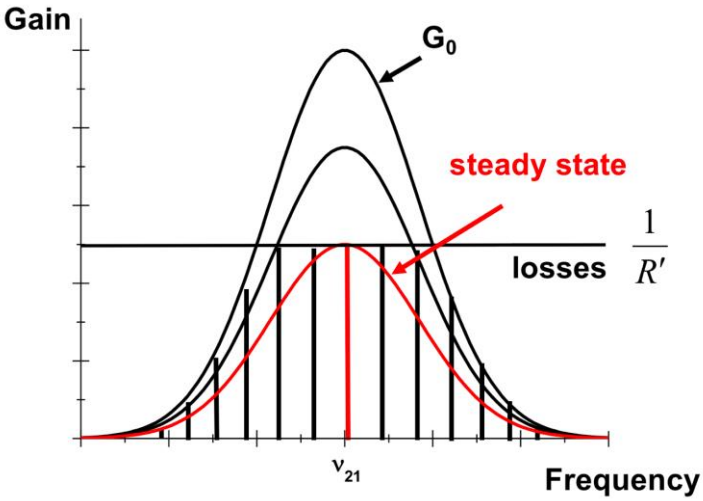

However, in reality, multi-mode operation and mode jumping can be observed even in the case of homogenously broadened transitions. The reason for this behavior is "spatial hole burning".

Spatial hole burning has its origin in a standing-wave pattern created inside a linear cavity for one or more oscillating modes. At the intensity maxima of the standing wave of a longitudinal mode the inversion is strongly reduced (i.e. "holes are burned" in the inversion profile along the z-axis / optical axis). This way the gain for this longitudinal mode is reduced due to saturation. At this point other longitudinal mode(s), with a standing-wave intensity pattern whose maxima partly overlap with the intensity minima of the standing wave of the old mode, might be preferred because their net-gain is larger (because at the position of their intensity maxima the inversion has not been strongly depleted). The result is a jump in operation between longitudinal modes and, finally, a multi-mode emission.

Which possibilities are there to avoid spatial hole burning?

One approach is the use of a ring cavity with a unidirectional operation. This configuration is referred to as a traveling-wave oscillator. In such an oscillator no standing wave can be created (due to the unidirectional propagation forced by the optical isolator). Without the standing-wave pattern spatial hole burning is suppressed and mode jumping is avoided. This, in principle, paves the way for single longitudinal mode emission in homogeneously-broadened lasers.

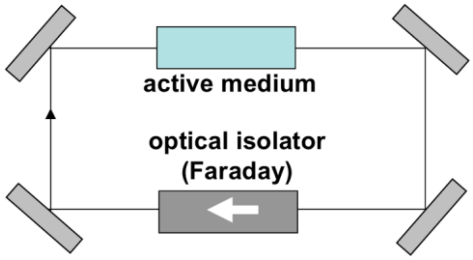

Additional approaches to control or reduce the number of longitudinal modes (also applicable to inhomogeneously broadened systems) are:

- force the laser to operate in the transverse fundamental mode.
- reduce the length of the resonator and, therewith, increase the mode spacing (FSR), which leads to fewer modes fitting below the spectral gain profile.
- reduce the pump power which, consequently, decreases the frequency bandwidth above threshold.
- integrate frequency-selective elements in the cavity, such as prisms, gratings or Fabry-Perot-etalons.

Fabry-Perot etalons allow for the highest frequency discrimination among the above listed options. A Fabry-Perot etalon consists of two parallel, partially reflective mirrors, e.g. on a glass plate. They are often slightly tilted to avoid the creation of sub-cavity effects. Their transmission characteristics are determined by a multi-beam interference (similar to the considerations done in a passive laser resonator).

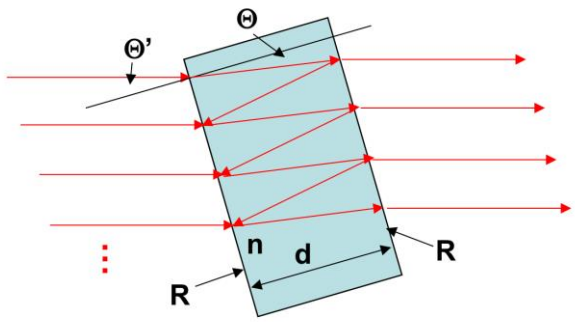

The maxima of transmission occur at frequencies which fulfill the condition that the path difference is a multiple of the wavelength (i.e. constructive interference):

$$n = m \cdot \frac{c}{2nd \cdot \cos Q}$$

The frequency separation between neighboring transmission maxima (FSR) is, therefore:

$$Dn = \frac{c}{2nd \cdot \cos Q} = FSR = \frac{1}{t_R} \qquad Dn \sim \frac{1}{d}$$

i.e. it is inversely proportional to the plate thickness. The bandwidth of each transmission maximum is given by the expression:

$$dn_{FP} = \frac{1}{F \cdot t_R} \quad with \quad F = \frac{p\sqrt{R}}{1 - R} \qquad \Rightarrow \quad dn_{FP} \sim \frac{1}{d}$$

The expression above indicates that the bandwidth is inversely proportional to the plate thickness as well. Thus, a thick etalon exhibits a small FSR and a narrow bandwidth of the transmission peaks. On the other hand, a thin etalon allows for a large FSR and a broad bandwidth of the resonances.

In the following the longitudinal mode selection in a dye laser, which can offer an extremely large gain bandwidth of several 100nm, is illustrated.

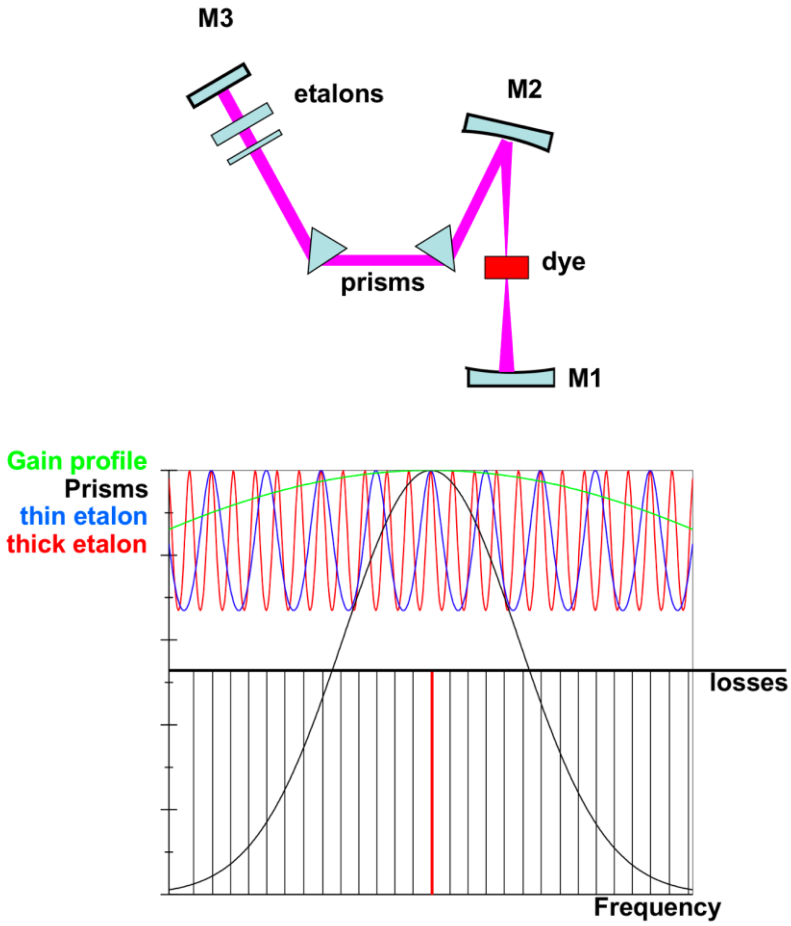

The green line illustrates the gain profile. Many longitudinal modes appear above the loss line. By adding a prism combination, as illustrated above, the number of modes above the loss line is already significantly reduced. Finally, a pair of etalons (thin + thick) with their tilt adjusted to overlap with the frequencies of the longitudinal modes finally create additional losses for all modes except for one, which becomes the only one able to oscillate.

5.8 Mode Locking – Generation of Ultra-short Laser Pulses

Q-switching has been discussed in chapter 4 as a method to generate short energetic pulses. However, pulses from a Q-switched laser cannot be ultra-short (i.e. they cannot have durations <10ps) as the propagation speed of the pulses in the cavity is limited (by the speed of light) and, therewith, an arbitrarily fast extraction of the inversion is not feasible.

The generation of ultra-short optical pulses is possible by means of mode-locking. The recipe for mode-locking is to ensure the simultaneous oscillation of many longitudinal modes and to couple them in such a way that they interfere destructively most of the time and constructively only for a short time.

In a laser resonator emitting a number of longitudinal modes with a statistical phase relation between them (this is actually the standard case), it is possible to observe a fluctuating intensity around an average value. Such an emission is nothing else than a statistical beating of multiple waves at different frequencies as illustrated in the plots below.

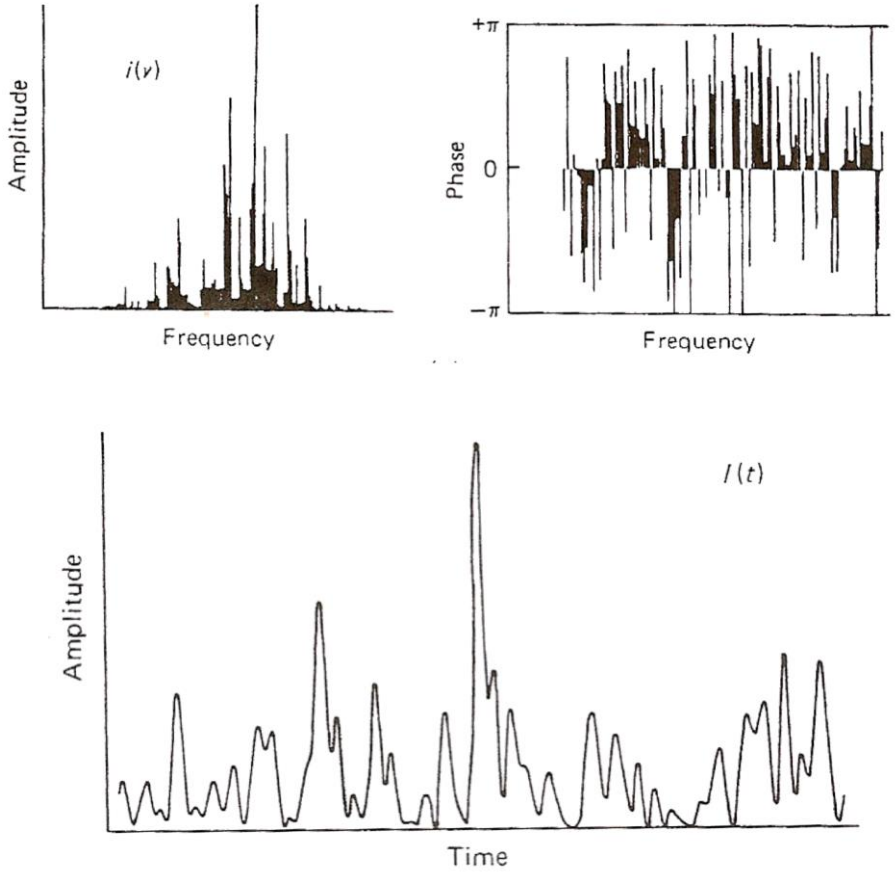

The mathematical description of such a multi-mode (i.e. multi-longitudinal-mode) emission at an arbitrary position z can be done by defining an electric field strength as:

$$E(t) = \sum_{n=-m}^{m} E_n \cdot \exp\left\{ i\left(\omega_0 + n\frac{2\pi}{t_R} \right) \cdot t + i \cdot \varphi_n \right\}$$

Where E_n is the E-field strength of the nth longitudinal mode and φ_n is the phase of the nth longitudinal mode. In the following, we simplify the mathematical treatment by assuming $\varphi_n = 0$ (i.e. all modes have the same phase, which is equal to 0) and $E_n = E_0$ (i.e. all modes have the same amplitude); With these assumptions the multi-mode emission is given by:

$$E(t) = E_0 \cdot \sum_{n=-m}^{m} \exp\left\{ i\left(\omega_0 + n\frac{2\pi}{t_R} \right) \cdot t \right\}$$

That expression is a finite series, which sum can be written as:

$$E(t) = E_0 \cdot \left[\frac{1 - \exp\left(iN \frac{2\pi}{t_R} t \right)}{1 - \exp\left(i \frac{2\pi}{t_R} t \right)} \right] \cdot \exp(i\omega_0 t) \quad ,$$

with $N = 2m+1$ being the total number of oscillating longitudinal modes. Thus the intensity of in-phase multi-mode emission (i.e. when all the longitudinal modes have the same phase) is:

$$I(t) \sim E(t) \cdot E(t)^* = E_0^2 \cdot \frac{\sin^2\left(N \cdot \pi \frac{t}{t_R} \right)}{\sin^2\left(\pi \frac{t}{t_R} \right)}$$

The following plot shows this intensity as a function of time for a resonator having a length of 15 cm (i.e. a cavity round-trip-time of 1 ns) and 5 longitudinal modes (N = 5) oscillating in-phase.

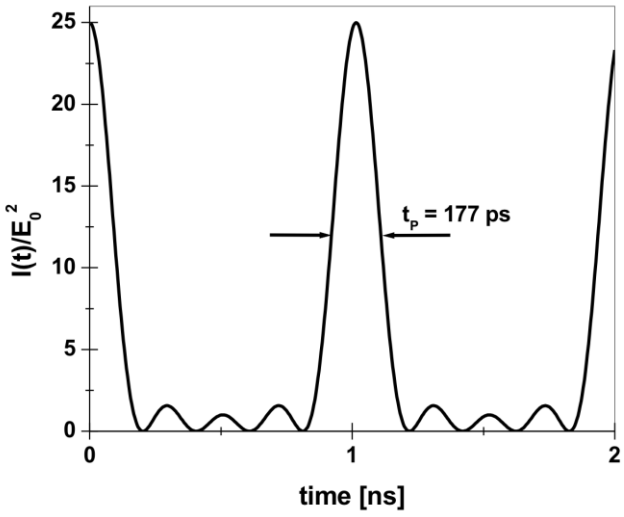

The plot reveals a pulse train with a repetition rate of 1 GHz. This, in turn, implies that there is only one pulse oscillating inside of the cavity.

The characteristic of such a multi-mode emission is similar to the spatial intensity pattern of multi-beam interference where N plays the role of the number of slits. It is clearly visible in the plot above that there are N-1/N-2 secondary minima/maxima. With an increasing number of N, the peaks/pulses get narrower and narrower and gain in intensity. At the same time the secondary maxima decrease in amplitude.

To get a rough estimation of the pulse duration, we can consider the distance from the peak of the pulse to the 1st minimum (both quantities are very comparable), which appears at:

$$N\pi \frac{t}{t_R} = \pi \quad \Rightarrow \quad t_{\min} = \frac{t_R}{N}$$

Thus, the pulse duration is approximately

$$t_P \approx \frac{t_R}{N} = \frac{1}{\Delta\nu},$$

with $\delta\nu$ being the spectral bandwidth of the emission.

This result is not surprising since we know from Fourier theory that a shorter feature in the temporal domain needs more spectral bandwidth. Hence, the shorter the pulse, the broader the bandwidth. In fact, for a given pulse shape, the product of the pulse duration and the spectral bandwidth is a constant known as time-bandwidth product (TBP: $t_P \cdot \delta\nu$). The shortest pulse for a given spectral bandwidth is called a transform-limited pulse and fulfills exactly the time-bandwidth product. The value of this product depends on the temporal shape of the pulse. Examples:

- *rectangular*: $t_P \cdot \delta\nu = 0.443$
- *Gaussian*: $t_P \cdot \delta\nu = 0.44$
- *sech²*: $t_P \cdot \delta\nu = 0.315$

On a different account, the peak value of the intensity of the in-phase multi-mode emission scales with:

$$I_{\max} \sim N^2 \cdot E_0^2.$$

In contrast, the temporally-averaged intensity of the emission of N modes with a statistical phase relation scales only with:

$$\langle I \rangle \sim N \cdot E_0^2.$$

5.9 Techniques of Mode-Locking

The main idea behind mode-locking is to ensure a preferred state of the laser in pulsed operation. This usually means that the cavity has lower losses in pulse operation than in continuous-wave emission. If this is achieved, a certain number of modes will automatically start to oscillate with a fixed phase relation.

As it was also the case in Q-switching, in the context of mode locking the different techniques can be classified in two main groups: active mode-locking and passive mode-locking.

Active Mode-Locking

Active mode-locking can be realized by using an intra-cavity modulator; it is used to modulate either the losses or the cavity length. It is important to note, however, that the modulation frequency has to be equal to the separation of the longitudinal modes.

A) modulation of losses

Let's focus the discussion, for the time being, in a single longitudinal mode of the laser centered at frequency ν. A sinusoidal amplitude modulation of the emission of said longitudinal mode with a frequency $\Delta\nu$ will generate side-bands with frequencies $\nu\pm\Delta\nu$. In turn, these new frequencies will also experience the modulation as well and will create new sidebands. If the sidebands fall at the frequencies corresponding to neighboring longitudinal modes (i.e. if the modulation frequency is equal to the inverse of the cavity round-trip time), then they can seed them and, thereby, imprint their phase on them. Thus, neighboring longitudinal modes will be locked (i.e. synchronized) in phase. In turn, through successive passes through the modulation, the side-band will generate new frequencies that will synchronize further longitudinal modes. This process continues until, at the end, all longitudinal modes within the gain profile are synchronized.

In the time domain the modulation frequency required to synchronize the longitudinal modes is equal to the inverse of the round-trip time. Hence, the oscillating electro-magnetic wave always sees an identical cycle of the loss modulation. This means that only radiation within the correct time-window can pass through the modulator (i.e. when it is at its low loss state). Consequently, the radiation gets more and more concentrated in short optical pulses (pulse shortening). However, such pulse shortening becomes less effective for shorter pulses.

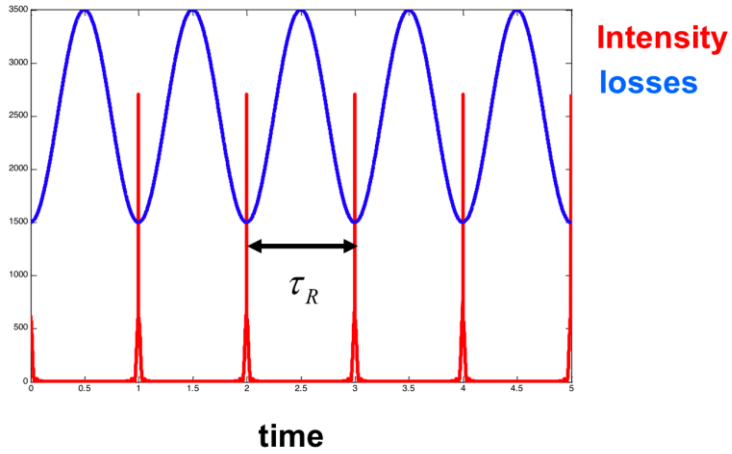

B) Phase modulation (also known as frequency-modulation mode-locking)

An electro-optical modulator allows for the modulation of the refractive index and, hence, of the accumulated phase of the light passing through it. However, a temporal change of the phase is equivalent to a frequency change of the light. In fact, the change of the instantaneous frequency is given by:

$$dw \sim \frac{\partial j}{\partial t}$$

Thus, if a sinusoidal modulation is applied to the electro-optical modulator with a repetition rate equal to the cavity round-trip time, the light in the cavity will be frequency-shifted (up or down). Consequently, repeated passes through an electro-optical modulator will end up shifting the radiation energy out of the gain bandwidth, unless

$$\frac{\partial j}{\partial t} = 0$$

is fulfilled. Therefore, modulations ultra-short optical pulses can appear at the maxima and minima of the phase. The drawback of this technique is that a random hopping between the two operation modes (i.e. min. and max.) can take place as illustrated below.

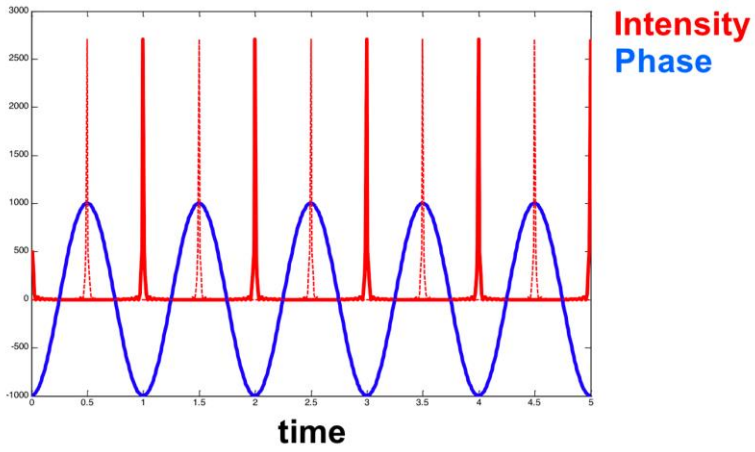

Passive Mode-Locking

The idea of passive mode-locking is that the pulse itself achieves the control of the loss modulation with frequency $1/\tau_R$. A mechanism is, therefore, needed which favors the pulsed mode against the continuous-wave mode (e.g. via a modulation of the Q-factor). Similar to Q-switching, such a loss modulation can be realized by an element with an intensity dependent reflectivity or transmission, as shown below.

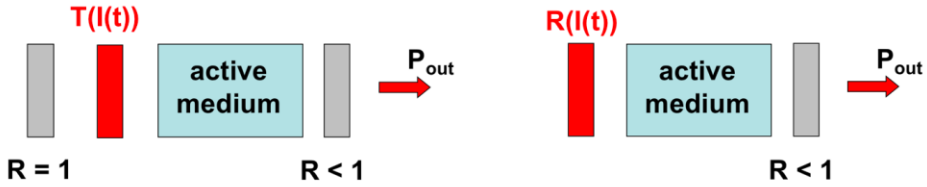

The following figure illustrates passive mode-locking and introduces the most relevant time scales. The lifetime of the high Q-factor (higher R), which is related to the recovery time τ_{rec} of the "modulator", has to be shorter than the cavity round-trip time τ_R, else just Q-switching is observed.

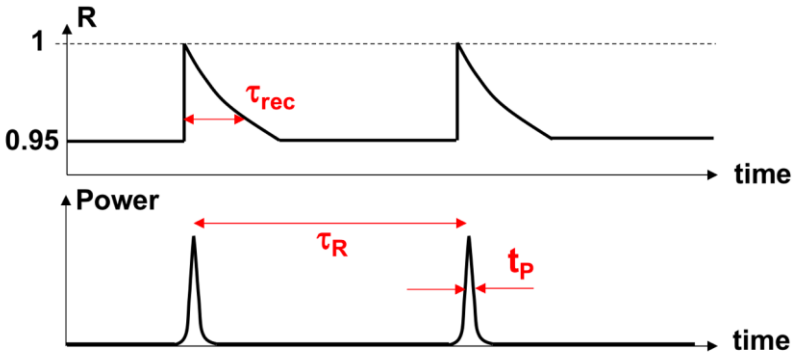

Saturable Absorbers

A saturable absorber can be regarded, in most cases, as a simple two-level system. In this 2-level system analogy, if the population density of the upper level approaches the population density of the lower level, the absorber is completely bleached and becomes transparent. If the recovery time (i.e. the time that it takes for the population in the excited state to transition back to the lower level) is longer than the pulse duration, we can assume that the entire pulse energy contributes to the saturation. In such cases, the reflectivity is considered to be a function of the fluence F_P, which is the pulse energy per area. A typical behavior is shown in the following figure.

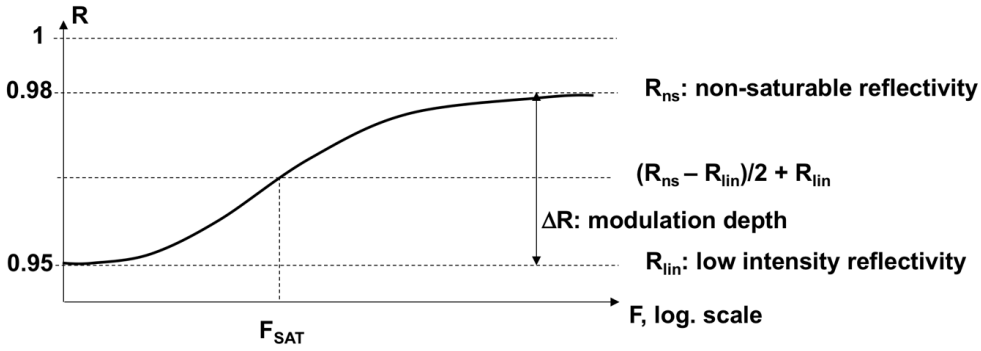

A prominent example of an absorber, often used in modern ultra-short pulse lasers, is the semiconductor saturable absorber mirror (known as SESAM), which is a semiconductor-based mirror structure with an incorporated saturable absorber layer. For example this can be realized with a semiconductor Bragg mirror (near the surface) placed behind a quantum-well absorber layer. Such SESAMs can be fabricated by molecular beam epitaxy (MBE). An interesting feature of these structure is that basically all relevant parameters (wavelength, bandwidth, F_{SAT}, t_{Rec}, ΔR, …) can be tailored by the design of the structure and by the absorber material.

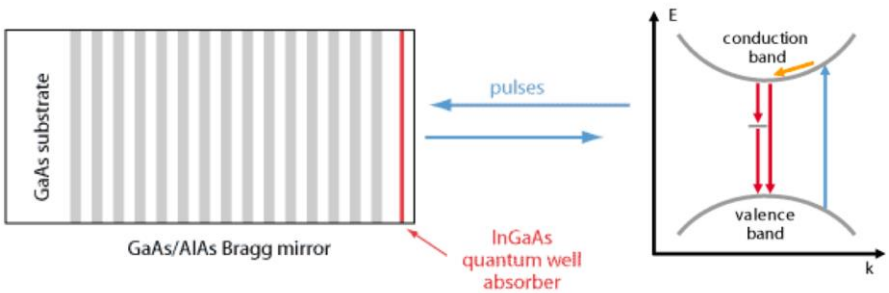

Kerr-lens mode-locking (KLM)

The refractive index of transparent materials is intensity-dependent (which is known as Kerr effect):

$$n(I) = n_0 + n_2 \cdot I$$

As the fundamental transverse mode (TEM_{00}) of a resonator has a Gaussian profile in the radial direction, a high intensity beam creates a gradient index lens in the active medium (i.e. a higher refractive index at the center of the beam). This leads to a nonlinear self-focusing of the beam and, therewith, for high intensities, to a reduction of the beam size at certain positions in the cavity. The focal length of such a Kerr-lens is given by:

$$f = \frac{\mathrm{p} \cdot w^4}{4 \cdot n_2 \cdot d \cdot P}$$

with w being the beam radius, d the length of medium, n_2 the nonlinear refractive index and P representing the peak-power of the pulse.

Hence, the Kerr-effect can be used, as illustrated below, as an intensity-dependent instantaneous modulator in a laser resonator (i.e. as an artificial saturable absorber), which can reduce the cavity round-trip losses for pulses with high peak powers.

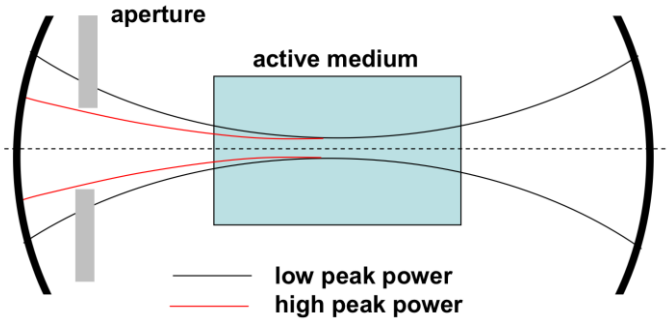

Additive Pulse Mode-Locking (APM)

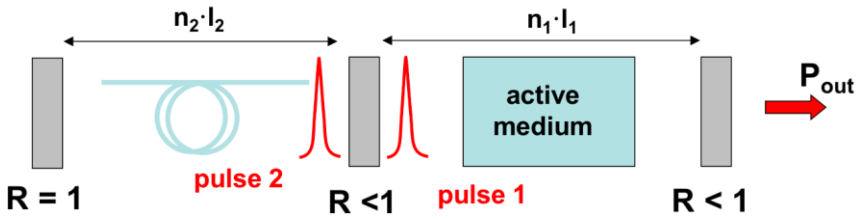

Additive pulse mode-locking comprises two coupled cavities (where pulse 1 travels in cavity 1 and pulse 2 in the second cavity) with matched round-trip times, i.e. $n_2 \cdot l_2 = n_1 \cdot l_1$. A nonlinear medium, e.g. an optical fiber, is placed in one of the cavities (e.q. cavity 2) in which the pulse collects a nonlinear temporal phase due to the temporal Kerr-effect (hereby the phase changes along the pulse).

After one round-trip, pulse 1 and pulse 2 interfere at the partly reflective mirror separating the two resonators. If the cavity lengths are adapted to ensure just constructive interference at the peak of the pulse, pulse shortening can be achieved.

The main disadvantage of this approach is the required interferometric stability of the setup, which makes APM ultra-short pulse lasers rather sensitive to external influences.

Time scales

Mode-locked lasers can generate pulses as short as 10 fs. The figures below illustrate how short such a pulse is compared to time scales humans are used to.

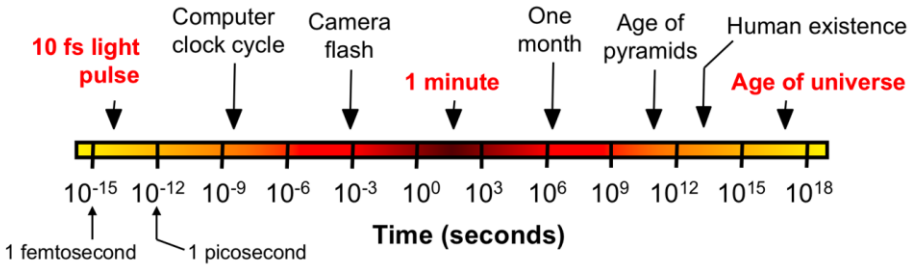

In fact, *such a pulse is to one minute what one minute is to the age of the universe!*

In 1 second light travels 7.5 times around the globe. Therefore, in 100 fs it will travel just 30 µm, which is comparable to the thickness of a human hair.